9-9-2010

# On the Use of Independent Component Analysis & Functional Network Connectivity Analysis: Evaluation on Two Distinct Large-Scale Psychopathology Studies

Michelle Juárez

Michelle Juárez
*Candidate*

Electrical and Computer Engineering
*Department*

This thesis is approved, and it is acceptable in quality and form for publication:

*Approved by the Thesis Committee:*

, Chairperson

Major Martinez

# ON THE USE OF INDEPENDENT COMPONENT ANALYSIS & FUNCTIONAL NETWORK CONNECTIVITY ANALYSIS: EVALUATION ON TWO DISTINCT LARGE-SCALE PSYCHOPATHOLOGY STUDIES

**BY**

**MICHELLE JUÁREZ**

**B.S., COMPUTER ENGINEERING**
**UNIVERSITY OF NEW MEXICO, 2007**

THESIS

Submitted in Partial Fulfillment of the
Requirements for the Degree of

**Master of Science**
**Computer Engineering**

The University of New Mexico
Albuquerque, New Mexico

**July 2010**

## DEDICATION

I dedicate this thesis to my grandmother, Angelita Ramírez, the eternal "brown-eyed girl." I miss you every day.

## ACKNOWLEDGEMENTS

I would like to thank my advisor and thesis chair, Dr. Vince D. Calhoun, for his patience, guidance, and un-ending support throughout my graduate academic career. He introduced me to this most challenging field of electrical and computer engineering. His professionalism, dedication to his research, and consideration of his staff and students are an inspiration and will remain with me as I set out onto new endeavors.

I would also like to thank my other committee members, Dr. Marios Pattichis, Dr. Vince Clark, and Dr. Kent Kiehl. Dr. Pattichis has been a constant source of encouragement and support since my undergraduate years. His dedication to his students truly shows and has been vital in my accomplishments thus far. Dr. Clark and Dr. Kiehl have generously lent their expertise in the field of psychology and provided invaluable contributions to the research in this study.

To my MIA labmates and colleagues, thank you for your assistance and guidance in my coursework and in my research, as well as for your amazing friendship.

To my mother, thank you for never giving up on me. I will never forget the sacrifices you have made for me throughout my life. And to my father, you continue to inspire me to achieve more and to be more, whatever it may be. I hope one day to be the adventurous globe-trotter that you are. And to my sisters, thank you for keeping me on my toes.

And finally, to my dearest friends and loved ones, you encouraged me to never give up, and you were my shoulders to lean on. Thank you for bringing the sunshine.

# ON THE USE OF INDEPENDENT COMPONENT ANALYSIS & FUNCTIONAL NETWORK CONNECTIVITY ANALYSIS: EVALUATION ON TWO DISTINCT LARGE-SCALE PSYCHOPATHOLOGY STUDIES

**BY**

**MICHELLE JUÁREZ**

ABSTRACT OF THESIS

Submitted in Partial Fulfillment of the
Requirements for the Degree of

**Master of Science**
**Computer Engineering**

The University of New Mexico
Albuquerque, New Mexico

**July 2010**

**ON THE USE OF INDEPENDENT COMPONENT ANALYSIS & FUNCTIONAL NETWORK CONNECTIVITY ANALYSIS: EVALUATION ON TWO DISTINCT LARGE-SCALE PSYCHOPATHOLOGY STUDIES**

**by**

**Michelle Juárez**

**B.S., Computer Engineering, University of New Mexico, 2007**

**M.S., Computer Engineering, University of New Mexico, 2010**

## ABSTRACT

Medical image analysis techniques are becoming ever useful in allowing us to better understand the complexities and constructs of the brain and its functions. These analysis methods have proven to be integral in revealing trends in brain activity within individuals with mental disorders that are distinguishable from what would be considered "normal" activity within healthy populations. This has led us to gaining a better understanding of functional connectivity within the brain, especially within populations suffering from mental disorders.

Functional magnetic resonance imaging (fMRI) is one of the leading techniques currently being implemented to explore cognitive function and aberrant brain activity resulting from mental illness. Functional connectivity has investigated the associations of spatially-remote neuronal activations in the brain. Independent component analysis (ICA) is the leading analytical method in functional connectivity research and has been

extensively implemented in the analysis of fMRI data, allowing us to draw group inferences from that data. However, there is mounting interest in the functional network connectivity (FNC) among components estimated through ICA. This type of analysis allows us to delve further into the temporal dependencies among components or "regions" within the brain. In this thesis, we investigate the implementation of group ICA and FNC analysis on two large-scale psychopathology studies – the first from a multi-site study involving the comparison of schizophrenia patients with healthy controls using a sensorimotor task paradigm, and the second from an investigation in psychopathy in prisoners performing an auditory oddball task. In both studies, we analyzed the fMRI data with group ICA and implemented FNC analysis on the resulting ICA output. The purpose of these studies was to investigate differences in modulation of task-related and default mode networks, identifying any potential temporal dependencies among selected components.

Our ultimate objective was to demonstrate the effective application of group ICA and FNC analysis together on two large-scale studies of two, distinct psychopathologies. The results of this combined method of analysis establish the practicality and general applicability of group ICA-FNC analysis in the growing fields of functional connectivity and functional network connectivity.

## TABLE OF CONTENTS

**LIST OF FIGURES** ..... **X**

**LIST OF TABLES** ..... **XI**

**CHAPTER 1 – INTRODUCTION TO THESIS** ..... **1**

INTRODUCTION AND MOTIVATION ..... 1
THESIS STATEMENT AND CONTRIBUTIONS ..... 5
THESIS SUMMARY ..... 7

**CHAPTER 2 – FMRI IMAGE ANALYSIS METHODS** ..... **9**

INDEPENDENT COMPONENT ANALYSIS ..... 9
Theory ..... 10
FUNCTIONAL NETWORK CONNECTIVITY ..... 13
Theory ..... 14

**CHAPTER 3 – SCHIZOPHRENIA** ..... **16**

INTRODUCTION ..... 16
METHODS ..... 18
Participants ..... 18
Task ..... 20
Imaging Parameters ..... 21
Data Analysis ..... 22
Independent Component Analysis ..... 22
Statistical Analyses ..... 24
FNC Analysis ..... 25
RESULTS ..... 26
Behavioral Results ..... 26
Selected Independent Components ..... 26
Comparison of Task-related Time Courses ..... 27
Correlations with Symptoms Scores and with Duration of Illness ..... 30
Site Differences ..... 31
FNC Analysis Results ..... 35
DISCUSSION ..... 36

**CHAPTER 4 – PSYCHOPATHY** ..... **43**

INTRODUCTION ..... 43
METHODS ..... 45
Participants ..... 45
Task ..... 47
Imaging Parameters ..... 49
Data Analysis ..... 49
Independent Component Analysis ..... 49
Statistical Analyses ..... 51
FNC Analysis ..... 53
RESULTS ..... 53

Comparison of Task-related Time Courses ..... 54
Correlations with PCL-R Scores ..... 57
Analysis of Frequency Spectra ..... 60
FNC Analysis Results ..... 61
DISCUSSION ..... 62
**CHAPTER 5 – CONCLUSION AND FUTURE WORK ..... 64**
CONCLUSION ..... 64
FUTURE RESEARCH TOPICS ..... 65
**REFERENCES ..... 66**

## LIST OF FIGURES

Figure 1: Group ICA model ..... 10

Figure 2: Auditory sensorimotor paradigm ..... 21

Figure 3: Regions of sensorimotor task-modulation ..... 27

Figure 4: Task-related modulation results based on one-sample t-tests ..... 30

Figure 5: Average magnitude and direction of beta weights, differentiated by site, for all subject test groups ..... 31

Figure 6: ICA time courses for all significant components ..... 32

Figure 7: Differences in task-related modulation among the subject test groups based on two-sample t-tests ..... 33

Figure 8: FNC results for healthy control subjects (top left), schizophrenia patients (top right), and the group differences detected between the two subject groups (HC – SZ) (bottom) ..... 36

Figure 9: PCL-R list items broken down by factor ..... 46

Figure 10: Auditory oddball paradigm sample sequence - the three different stimuli are represented by different shapes and are unevenly-spaced to demonstrate the pseudorandom presentation ..... 49

Figure 11: Regions of auditory oddball task-modulation ..... 56

Figure 12: Associated time courses for the significant components ..... 57

Figure 13: FNC results for low PCL-R subjects (left) and high PCL-R subjects (right) .. 62

## LIST OF TABLES

Table 1: Subject demographics at intake ..... 20

Table 2: Statistical results of sensorimotor data ..... 29

Table 3: Talairach coordinates for the group ICA ..... 34

Table 4: Psychopathy demographics and PCL-R scores ..... 47

Table 5: Results from the one and two-sample t-tests performed on the beta weights, broken down by PCL-R subject group ..... 55

Table 6: Correlations of the beta weights with PCL-R total scores for the normal ICA .. 58

Table 7: Correlations of the beta weights with PCL-R factor 1 scores ..... 59

Table 8: Correlations of the beta weights with PCL-R factor 2 scores ..... 60

Table 9: Correlations of the time course frequency spectra with the factor 1, factor 2, and total PCL-R scores ..... 61

# CHAPTER 1 – INTRODUCTION TO THESIS

## INTRODUCTION AND MOTIVATION

Mental disorders are defined as patterns of psychological or behavioral activity in an individual that are deemed as abnormal and are not part of the normal, healthy development of the brain or psyche. Mental illness can develop and progress for a variety of reasons, including, but not limited to: genetic predisposition, traumatic brain injury, traumatic experience, stress, brain degeneration, substance abuse, disease, etc. Quite often, mental disorders occur as a result of a combination of triggers, and there is a general consensus that no one particular source or cause can be established for the development of a disorder. However, we understand that both genetics and environmental factors together play a role in the development and progression of these types of disorders.

More than one-third of people worldwide report having experienced at least one mental disorder in their lives (2000). In the United States alone, that number jumps to almost half the population suffering from a mental disorder at least once in their lifetimes (Kessler et al., 2005). Despite the high prevalence of mental illness worldwide, these disorders are often misunderstood and/or are difficult, if not seemingly impossible, to treat. This is understandable given the various types of disorders currently classified and the diversities consisting within each type. As a result, there have been several continued attempts over the centuries to research, document, and diagnose the origins and epidemiology of mental disorders. Thus, the field of neuroscience was born.

Several research methods have been developed to better understand the cognitive functions of the brain. Many of these involved the documentation of behaviors and

symptoms related to both healthy and dysfunctional mental health. In addition to this documentation, the majority of brain research consisted of anatomical studies of the physical brain. Until these most recent decades, these research methods had their many limitations, primarily due to the primitive technology in existence at the time. However, thanks to the strides we have made in advancing our computer and imaging technology, it is now possible to directly study the cognitive brain in ways that would be nearly impossible using the former anatomical approach. The field of neuroimaging involves the use of medical imaging techniques to study the changes or variations in brain structure or function/activation and how they correlate to documented aberrations in behavior and cognition. And, one of the leading imaging methods that is increasingly and extensively used is functional magnetic resonance imaging.

Functional magnetic resonance imaging (fMRI) is a method of brain imaging that measures the blood oxygen level dependent (BOLD) changes in the brain in response to a given task. This is also known as the hemodynamic response. The signals extracted during the MRI scans can then be processed and analyzed in a variety of ways to indirectly obtain information on the location and modulation of possible neuronal activity that occurred within the subjects' brains either during rest or in response to a task. The need for more efficient, accurate, and informative methods for the analysis of fMRI data has led to the development of a variety of techniques in the study of "functional connectivity."

Functional connectivity is defined as the study of the correlations between neuronal activations between spatially-remote regions within the brain (Friston, 1994). In the field of neuroimaging, statistical analyses is performed on the time series of imaging

data collected from subjects who are either at rest or who perform a cognitive task. Early analysis studies on functional connectivity consisted of the correlation of seed voxels (volumetric pixels within the 3D space of the brain) within particular functional regions in the brain with fMRI time courses, after which differences between these correlations were analyzed (Biswal et al., 1995; Biswal et al., 1997; Cordes et al., 2002; Cordes et al., 2001; Cordes et al., 2000; Lowe et al., 1998).

However, the introduction of independent component analysis (ICA) greatly transformed the field of functional connectivity (Calhoun et al., 2001b, c; McKeown et al., 1998). When applied to fMRI data, ICA is a multivariate method of analysis that works to separate and reconstruct linearly-mixed signals, which is similar in nature to the separation of different voices recorded by a single microphone, as in the "cocktail party" problem (Bell and Sejnowski, 1995; McKeown and Sejnowski, 1998). Taking these recovered signals, ICA determines a set of maximally-dependent "components" (Calhoun and Adali, 2006). Assuming that the brain consists of a set of sparse, spatially-independent functional networks, ICA works to reveal and distinguish these networks, associating each with its own specific time course. ICA characterizes each network it reveals as a maximally-independent component in its output. In essence, each component is a functionally connected network consisting of a set of voxels within the brain that have the same time course and exhibit a temporally coherent signal (Calhoun et al., 2009a). Benefits to this analysis technique include (yadda). Group ICA improved on the original method of ICA by expanding the application of this technique to group studies, allowing us the ability to make group inferences from a collection of data from several subjects (Calhoun et al., 2001b). Thus, taking the components output from group ICA, we

are able to draw group inferences on the functional networks discovered based on a series of statistical analyses on the voxels and time courses characterized by each component. These group inferences allow us to characterize trends in modulation that distinguish the cognitive performance of those with a mental disorder from a healthy population.

While group ICA has been effective in revealing trends in modulation related to the functional connectivity, it does not address the existence of possible temporal relationships among those spatially-independent networks. These temporal relationships are the weaker dependencies that may exist among distinct components identified by ICA. These dependencies, though significant, are considerably weaker than the dependencies between regions found within a particular component, thus preventing the distinct components from being combined as a single component (Calhoun et al., 2003). The temporal dependencies among components revealed through ICA are defined as the "functional network connectivity" among these components (Jafri et al., 2008). Functional network connectivity (FNC) is a relatively new topic of research that goes beyond functional connectivity by focusing on the functional integration among different brain regions and examines the interactions among these regions. These interactions may provide information on how activity in one region of the brain may affect the activity in one or more other regions. The motivation behind investigating these temporal dependencies is to better understand how activity in one region or component network may affect or even instigate activity in another completely separate region in the brain. FNC analysis allows us to describe the temporal dependencies between the components revealed through group ICA, depending on the method implemented. There are several

approaches to the study of the dependencies among components. However, this thesis will focus on the group correlation approach toward these temporal relationships.

## THESIS STATEMENT AND CONTRIBUTIONS

In this thesis, I will demonstrate the application of two fMRI image analysis techniques, group ICA and FNC analysis, on two very different psychopathology studies. Previously, no other schizophrenia studies into the sensorimotor network have been conducted on such a large scale. Additionally, this is the first study known to not only reveal through ICA specific and distinct sensorimotor networks implicated in schizophrenia, but also examine the group differences in task modulation between patients who vary greatly in their duration of illness and a demographically-matched healthy control population.

Imaging research into the cognitive dysfunctions involved in psychopathy has been very limited for a variety of reasons. Psychopathy as a mental disorder can be very difficult to diagnose, and the behavioral symptoms exhibited can vary greatly, depending on the psychopathy checklist revised (PCL-R) clinical scoring of the individual (Hare, 1991). It is well-known that many prisoners incarcerated for serious crimes suffer from some degree of psychopathy, but gaining safe access to such individuals for the purpose of neuroimaging research has been nearly impossible until very recently. The psychopathy study highlighted in this thesis is innovative in its data collection approach in that it uses fMRI data collected via a mobile MR scanner that was taken directly to a New Mexico prison site. As a result, we were able to collect functional imaging data from a large pool of psychopathy subjects with a wide range of PCL-R clinical scores. To

date, this is the first large-scale fMRI study of psychopathy subjects that not only reveals distinct functional networks from an auditory oddball task, but also shows group differences in modulation based on the PCL-R scoring of subjects.

FNC analysis is a relatively new field of imaging research that is beginning to gain interest within the neuroimaging community. Though group ICA has been effectively implemented to reveal functional networks within the brain that may be implicated in particular psychopathologies, information on how these network components interact with one another is relatively unknown. These interactions, or temporal dependencies, among distinct brain regions may essentially be the cause for dysfunctional communication among those same distributed brain regions, resulting in the functional deficits of the particular mental disorder. Research into FNC has been very limited, and to date, there are no known studies that have investigated FNC in the sensorimotor network of schizophrenia or in psychopathy, especially on such a large scale. Because FNC analysis does not require additional data collection or analysis other than the data already acquired through fMRI scans and analyzed through group ICA, it is the next logical and easily implemented step in fMRI research. The application of both group ICA and FNC analysis together may provide in-depth information not only on functional brain networks implicated in a variety of psychopathologies, but also reveal clues on the temporal dependencies and interactions of these distinct brain regions to better characterize the cognitive dysfunctions observed within individuals suffering from mental disorders.

## THESIS SUMMARY

Chapter 1 of this thesis introduced the topic of mental illness, in particular schizophrenia and psychopathy, and the current approaches being implemented in combating these diseases. It discussed how fMRI image analysis techniques have become increasingly vital in understanding the cognitive functions of the brain and introduced the topics of functional connectivity and functional network connectivity in fMRI research. Finally, it detailed how the implementation of group ICA and FNC analysis together can effectively address the questions posed by these research topics.

In Chapter 2, we will present background information on the two image analysis methods highlighted in this study – group ICA and FNC analysis. We will provide detailed information into the technical theory behind each method and discuss how, when implemented together, they can provide an extra dimension of understanding in how the networks implicated in an illness interact and affect one another. We will show how this knowledge is the next logical step needed in understanding causality among brain networks.

In Chapter 3, we will demonstrate the application of group ICA and FNC analysis on fMRI data collected in a large-scale, multi-site research study comparing the brain modulations of schizophrenia patients with healthy controls. After providing some extensive background information on the subject of schizophrenia and the benefits of using a robust sensorimotor paradigm, we will show how ICA was effective in revealing several distinct networks within the brain that demonstrated high task-modulation and showed significant differences in that modulation between patients and controls. In addition, we show how that modulation correlates with the duration of illness within the

patient group. We will then provide the results of the FNC analysis and discuss the possible implications regarding causality among the networks.

In Chapter 4, we will again demonstrate the application of these analysis tools on fMRI data collected from subjects diagnosed with psychopathy. We will provide an extensive introduction to the topic of psychopathy and the rating of the severity of this disorder in subjects through PCL-R scoring. As well, I will discuss the aspects of the auditory oddball paradigm. We will next provide the results of the ICA and FNC analysis, demonstrating not only the trends and differences in modulation among groups with different PCL-R scores, but also the potential temporal dependencies among the networks identified.

Chapter 5 will bring this thesis to a close with a discussion of the conclusions that we established from the two research studies implementing group ICA and FNC analysis. We will also introduce potential topics for future investigation in the development of improved versions and implementations of these analysis tools.

# CHAPTER 2 – FMRI IMAGE ANALYSIS METHODS

## INDEPENDENT COMPONENT ANALYSIS

Independent component analysis (ICA) is a multivariate method of analysis to measure the functional connectivity of spatially distinct regions within the brain. Assuming a set of linearly mixed signals stemming from statistically independent hemodynamic sources, it works decompose and separate these signals from one another. Based on those signals, it determines a set of spatially distinct and temporally coherent components consisting of regions or networks within the brain that exhibit a BOLD response that is either task-related or resulting from brain activity during rest.

In group ICA, we expand this analysis method to take in raw fMRI data from several subjects to not only produce components and time courses that are combined across subjects, but also still maintain the ability to examine the individual time courses generated for each subject in the study. It is from these group components and time courses that we are able to make group inferences about the hemodynamic responses observed and compare how these responses may differ among groups of subjects within a single study. This allows us to comparatively explore the functional connectivity of subjects with a particular mental disorder against a healthy population or with other groups of individuals with varying degrees of dysfunction.

Next, we provide a background on the theory behind the processes involved in group ICA, as developed by Calhoun et al (Calhoun et al., 2001b).

## Theory

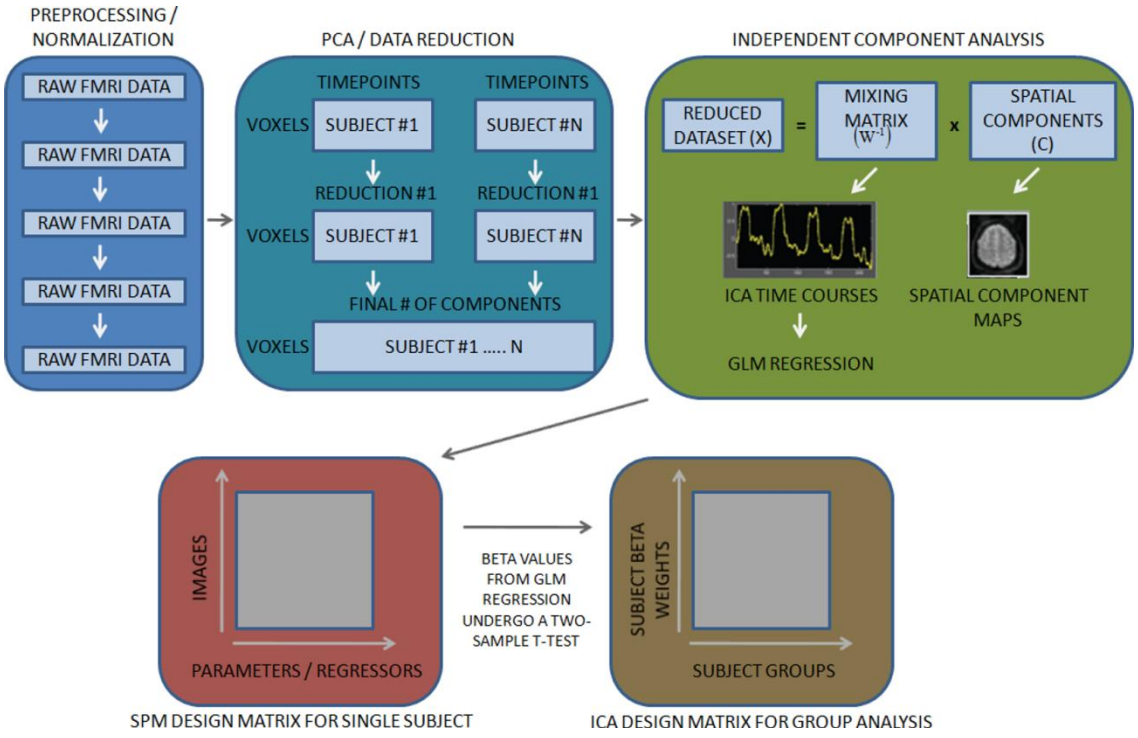


Figure 1: Group ICA model

In Figure 1, we examine the various steps and processes involved in group ICA. The entire system can be broken down into two primary blocks consisting of sequential procedures: the data acquisition block and the post-processing and analyses block. During data acquisition, raw fMRI data is collected from subjects who undergo an fMRI scan. These test subjects are either at rest (for resting-state studies) or perform a specific task (for cognitive function studies) according to a pre-determined task design paradigm. Assuming a set of statistically independent hemodynamic source locations within the brain, for *M* total test subjects and *N* total sources within the brain,

$$s_i(v) = \left[s_1(v_p), s_2(v_p), \ldots, s_N(v_p)\right]^T \tag{1}$$

$s_i(v)$ represents the $i^{th}$ source at a location $v$ for the $p^{th}$ test subject. Each source has a weight attributed to it based on how much that source contributes to a voxel within the brain's 3D space. Each weight is multiplied by the time course associated with its particular source. Assuming that each voxel is a linear mixture that is the summation of all sources contained within the brain of a subject, we can derive a sampling of these source signals contained within system **A** in the brain via Equation 2.

$$u_i(v) = [u_1(v_p), u_2(v_p), ..., u_N(v_p)]^T \tag{2}$$

The first step in data acquisition is to collect raw imaging data from all *M* subjects via an fMRI scan. During each scan, there is a total of *K* discrete time points during which we discretely sample the hemodynamic responses produced in the brain. For a set number of voxels, *V*, this sampling is described by Equation 3.

$$y_p(i_p) = [y_1(i_p), y_2(i_p), ..., y_K(i_p)]^T \tag{3}$$

Once this sampled fMRI data is collected, we enter the post-processing and analyses stage in the ICA system model. In this stage, the raw data is run through a series of processes and analyses, resulting in a set of grouped components to represent the collective modulation observed in all subjects. The first step in this stage is the preprocessing and spatial normalization of data into a standard space (Talairach and Tournoux, 1988). Next we perform data reduction through principal component analysis (PCA) to minimize the computational load during ICA (McKeown et al., 1998). This is followed by the actual ICA, in which we estimate a set of independent components. In the final stage of the post-processing and analyses block, a set of group maps and time courses are generated by grouping and thresholding the components estimated during ICA across all subjects (Calhoun et al., 2001b).

Because we initially assumed during data acquisition that imaging data from each scanned subject are statistically independent from that of the other subjects, we can derive the joint probability density function (pdf) to represent the statistical observations of the source signals collected from each subject in the population of all subjects in a study. This allows for the separability of the unmixing matrix that is generated during group ICA.

In order to estimate the number of components to be output during ICA, we must first estimate the total number of sources from the aggregate set of subjects and reduce the magnitude of the data collected. Source estimation is accomplished through the minimum description length (MDL) criterion (Rissanen, 1983). PCA decomposition is the method by which we reduce the dimension of the aggregate data collected from all subjects. Again, the MDL criterion determines the dimension to which we can effectively reduce this data for the final estimation of the number of components to be output by group ICA.

The next step in the post-processing stage of ICA is to estimate and produce a set of "group" components that is identical across all subjects, such that group inferences may be interpreted from the results. This is accomplished by performing ICA on all subjects and only estimating one set of components. As described previously, data reduction must be performed prior to the application of ICA. This occurs in two stages – first, the dimension of the data collected from each individual is reduced and then concatenated for all subjects; next, the concatenated data is further reduced into an aggregate mixing matrix, from which we can back-reconstruct the ICA maps for each, individual subject. As stated previously, the unmixing matrices used in back-

reconstruction are separable across all subjects because the dependence among the signals is minimal.

As part of the back-reconstruction stage of group ICA, we generate spatial maps and time courses that represent the hemodynamic response observed during the scan. The time courses generated for individual subjects may be averaged across a set of subjects to create a time course that represents the modulation of that particular group. Finally, the group ICA maps generated must be thresholded through the reconstruction of the individual ICA maps. These single-subject maps are reconstructed from the group ICA maps via a "random effects" inference that is made on a set of random variables consisting of the magnitudes and weights of the voxels found within the ICA components. These random variables are then subjected to a one-sample t-test, in which the hypothesis is null (zero magnitude).

## FUNCTIONAL NETWORK CONNECTIVITY

While group ICA is essential in revealing trends in dysfunction within the components associated with the brain regions/networks implicated by a BOLD response, it does not provide information on the relationships among these components. Functional network connectivity expands on the study of functional connectivity by investigating the weaker temporal relationships among the time courses generated for the functional networks revealed by group ICA. Even though the components estimated through ICA are spatially independent and distinct, there may exist weaker temporal dependencies among these components that can affect the hemodynamic responses among networks, which is the key theory behind causation.

There are a few methods that have been developed to investigate these temporal relationships among components. However, the method implemented in this thesis is the maximal lagged correlation method, wherein we perform a correlation among all the pair-wise combinations of the time courses for each component to identify trends in the hemodynamic latency among the networks. Next, we provide a background on the theory behind the processes involved in FNC analysis, as developed by Jafri et al (Jafri et al., 2008).

**Theory**

The first step in the FNC analysis process is the implementation of group ICA on a set of test subjects, estimating a series of independent components from the processed fMRI data collected. Once these components are generated, components of interest must be systematically selected from the entire set of estimated components. Selection of these components is based on how much a particular component is associated (correlated) with task-modulated activation (indicating association with a hemodynamic response in gray matter), cerebral spinal fluid (CSF), white matter, or is an artifact. Artifactual components can be generated through head motion or eye movements during a scan and/or caused by blood pulses at the base of the brain. Components that are not associated with signal changes within the brain's gray matter are generally discarded from further analyses.

Once the number of components has been reduced to only include components of interest, the time courses for these components are filtered to remove any residual noise. After noise removal, the total number of pair-wise combinations among the time courses for these components is calculated. These correlations will indicate how similarly any

two components were modulated by the task, indicating a potential association in the hemodynamic response between the two regions being compared. So, for a given number of components of interest, *n*, each with its associated time course, the total number of pair-wise combinations would be:

$$\binom{n}{2} \tag{4}$$

The maximal lagged correlation is performed on each of these pair-wise combinations of time courses. The mathematics behind this correlation are given in Equation 5.

$$\rho_{\Delta i} = \frac{\left(\overline{X}_{i_0}^{T}\right)\left(\overline{Y}_{i_0+\Delta i}\right)}{\sqrt{\left(\overline{X}_{i_0}^{T}\overline{X}_{i_0}\right)} \times \sqrt{\left(\overline{Y}_{i_0+\Delta i}^{T}\overline{Y}_{i_0+\Delta i}\right)}} \tag{5}$$

To calculate the correlation, $\rho$, between any two time course pairs, we are given the total number of time points for the time courses, *T*. Each time course is assigned a dimension, $\overline{X}$ or $\overline{Y}$, each with a starting reference of $i_0$, with the time change in seconds, $\Delta i$. *Y* is circularly shifted by $\Delta i$ from its reference point. $\Delta i$ thus represents the lag between the two time courses $\overline{X}_{i_0}^{T}$ and $\overline{Y}_{i_0+\Delta i}^{T}$. The maximal correlation and its corresponding lag time are saved for each of the two time courses for later analysis.

## CHAPTER 3 – SCHIZOPHRENIA

### INTRODUCTION

Models of cognitive dysfunction in schizophrenia focus on bottom-up and top-down pathophysiological models of brain dysfunction. Previous studies have shown that patients with schizophrenia have deficits in basic sensory and motor processing consistent with a model of bottom-up and top-down cognitive deficits (Braff and Saccuzzo, 1981; Holzman et al., 1974; Javitt, 2009; Nuechterlein et al., 1994; Saccuzzo and Braff, 1981). The consequences of basic auditory sensory processing deficits will have upstream consequences such as deficits in attention, phonetic and prosodic processing (Javitt, 2009). Both bottom-up and top-down deficits in sensory processing may result in impaired cognition and low quality of life for afflicted patients with schizophrenia (Green et al., 2000).

Cognitive dysfunction in schizophrenia may be related to failures in coordination of brain regions (Ford and Mathalon, 2008; Friston and Frith, 1995). The application of group independent component analysis (ICA) to fMRI data is a method of assessing the coordination of components or neural networks in the temporal domain. The components identified by group ICA are understood to be functionally connected regions or temporally coherent networks within the brain.(McKeown et al., 2002). Each spatially independent component has a respective time course that can be regressed with a model of the hemodynamic response for a particular cognitive paradigm. The resulting beta weights provide a measure of task-related connectivity and allow for group comparisons (Calhoun et al., 2001b).

Previous investigators have used the ICA time course to test for aberrant connectivity in schizophrenia (Garrity et al., 2007; Kim et al., 2009a; Kim et al., 2009b). The fMRI paradigms have included the auditory oddball discrimination task (novelty detection paradigm) and the Sternberg item recognition paradigm (working memory). These studies have consistently shown less positive modulation of task related networks in the patients with schizophrenia. The affected networks have included working memory (dorsolateral prefrontal cortex), motor (cerebellar), and auditory (temporal lobes) functions. The default mode of brain function is defined as a baseline condition in which the brain is in a resting state (Raichle et al., 2001). In contrast to the task-related networks, the default mode network is typically active during rest and decreases during an attention-demanding task. Previous studies have also shown that the patients with schizophrenia have less modulation of the default mode network relative to controls (Garrity et al., 2007; Kim et al., 2009a; Kim et al., 2009b). Aberrant connectivity with both task-related and default mode networks may be particularly relevant to the pathophysiology of schizophrenia (Williamson, 2007).

The goal of the present study was to apply ICA to assess potential differences in functional connectivity between patients with schizophrenia and healthy controls during a basic, auditory sensorimotor task. This study is, to our knowledge, the first application of ICA to uncover distinct sensory and motor networks that are affected by the onset and progression of schizophrenia. We use a simple and robust auditory paradigm initially developed as a calibration task in multi-center fMRI studies (Friedman et al., 2008). Based on prior studies that show patients with schizophrenia are impaired in basic sensorimotor processes, we hypothesized that patients with schizophrenia would have

less task-related modulation in auditory, sensorimotor, and default mode networks. We also compare the effect of duration of illness on the functional connectivity of these networks. We hypothesized that increased duration of illness will be associated with a further reduction of task-related modulation of these respective networks. These abnormalities would suggest basic information processing deficits in patients with schizophrenia.

## METHODS

### Participants

The Mind Clinical Imaging Consortium (MCIC) is a multisite, collaborative effort of four investigative teams from New Mexico, Minnesota, Iowa, and Massachusetts. The primary goal of this consortium was the study of the neural mechanisms of schizophrenia patients who were at various stages of illness. This collaborative, multisite design allowed for the collection of data from a large pool of both healthy control subjects and patients with schizophrenia. Participants consisted of 122 patients with schizophrenia and 145 matched healthy controls. The breakdown by site is as follows: New Mexico (32 patients, 38 healthy controls), Iowa (35 patients, 56 healthy controls), Minnesota (30 patients, 26 healthy controls), and Massachusetts (25 patients, 25 healthy controls). We further subdivided the patient group using a median split into two equal-size groups based on the patients' duration of illness (DOI). The sole purpose for this split during the analysis of the collected data was to evaluate whether both groups showed similar directionality in task modulation. The patients were recruited from clinics, inpatient units, group homes or vocational training programs, and from referrals from community

physicians. Controls were recruited from the local community through newspaper advertisements and through fliers. All healthy control subjects were screened to rule out any medical, neurological, or psychiatric illnesses, including any history of substance abuse.

Diagnoses were based on a DSM-based interview using either the Structured Clinical Interview for DSM-IV-TR Disorders (First et al., 1997) or the Comprehensive Assessment of Symptoms and History (Andreasen et al., 1992). Inclusion criteria for our schizophrenia patients included diagnoses of schizophrenia, schizophreniform disorder, or schizoaffective disorder. Measures of positive and negative schizophrenia symptoms were obtained using the Scale for the Assessment of Positive Symptoms (SAPS) (Andreasen, 1984) and the Scale for the Assessment of Negative Symptoms (SANS) (Andreasen, 1983), respectively. Patients with schizophrenia ranged in age from 18 to 60 years of age. These patients were taking either first generation antipsychotic or atypical medications. All subjects were age and sex-matched, and the healthy controls span the full age range of the patients (including the patients with a shorter DOI). All were fluent in English. A breakdown of the demographic and clinical data is provided in Table 1.

| | All Patients | All Healthy Controls |
|---|---|---|
| **Average Age / Standard Deviation** | 33.8 yrs / 11.2 SD | 31.7 yrs / 11.3 SD |
| **Gender** | 93 M / 29 F | 87 M / 58 F |
| **Handedness** | Right: 106<br>Left: 4<br>Ambi: 8 | Right: 133<br>Left: 7<br>Ambi: 4 |
| **Parental SES** | 2.81 | 2.67 |
| **SAPS Average / Standard Deviation** | 4.6 / 2.9 SD | N/A |
| **SANS Average / Standard Deviation** | 7.6 / 3.7 SD | N/A |

Table 1: Subject demographics at intake

**Task**

In order to robustly activate the auditory cortex, participants were presented with a series of audio tones of varying frequencies. This task used a block design paradigm in which the auditory stimuli were presented to each participant over the course of two runs while undergoing the fMRI scan. Within each run there were 15 blocks, each with duration of 16s on and 16s off. For the duration of the on-block, 200 msec tones were presented with a 500 msec SOA (stimulus onset asynchrony). During a test scan, the volume was calibrated to ensure that all test subjects were able to hear the tones comfortably over the background noise of the actual scanner. Consequently, the volume of the tones varied depending on the subject's degree of hearing during the audio setup for the task, therefore minimizing any auditory signal differences among groups with different hearing capabilities.

The auditory scale consisted of 16 different tones, ranging in frequency from 236 Hz to 1318 Hz. The first tone presented within a given block was set at the lowest pitch. Each tone that followed was at a higher pitch than the previous, creating a stair-step pattern of tones, which rose to a peak, followed by a symmetric descent. The participant was instructed to press the right thumb of the MIND input device (http://www.mrn.org/mind-input-device/index.php) each time after hearing each individual tone. This pattern of ascending and descending scales continued for the duration of the 16 sec block. The total duration of each run was 240 sec (120 TRs, TR = 2000 msec). Prior to execution of the task in the scanner, all subjects practiced performing this task to ensure capability in completing it correctly. This was done either on a computer in a console room or in a mock scanner session.

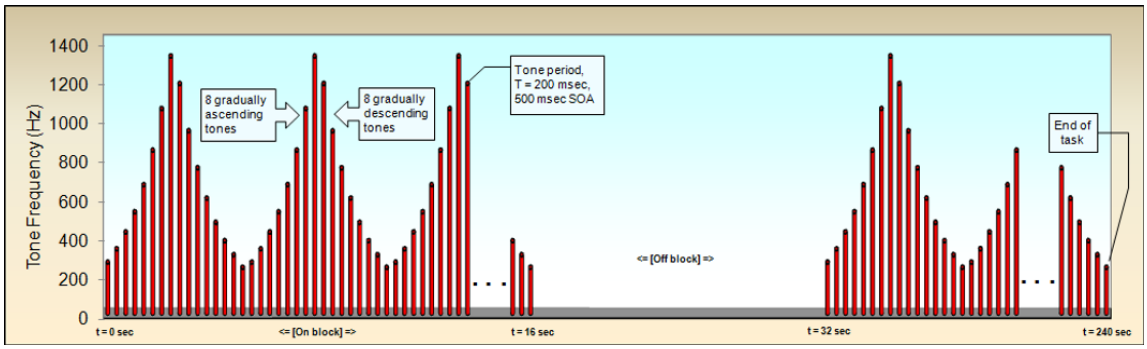


Figure 2: Auditory sensorimotor paradigm

## Imaging Parameters

Functional data were acquired at all four sites with EPI sequences on Siemens scanners at 3.0 Tesla (T), except at the New Mexico site where a 1.5T scanner was used. The imaging sequence parameters for these functional scans are as follow: Pulse sequence = PACE-enabled, single shot, single echo EPI, scan plane = oblique axial, AC-PC, copy T2 in-plane prescription, FOV = 22 cm, 27 slices, slice thickness = 4mm, 1 mm

skip, TR = 2000 ms, TE = 30ms (3.0T); 40ms (1.5T), FA = 90 degrees, BW = ±100 kHz =3126 Hz/Px, 64×64 matrix, 1 shot.

**Data Analysis**

*Preprocessing:* FMRI data were preprocessed using the SPM5 software package. Images were motion-corrected using INRIalign – an algorithm unbiased by local signal changes (Freire and Mangin, 2001; Freire et al., 2002). Data were spatially normalized into the standard Montreal Neurological Institute space (Friston, 1995) and slightly sub-sampled to 3×3×3 mm, resulting in 53×63×46 voxels. Next the data were spatially smoothed with a 10×10×10 mm full width at half-maximum Gaussian kernel. The resulting coordinates were converted to the Talairach and Tournoux standard space for anatomical mapping (Talairach and Tournoux, 1988).

**Independent Component Analysis**

Following the SPM5 preprocessing, a group ICA was performed on the preprocessed data (Calhoun et al., 2001b). The methods prescribed by this process were performed via the group ICA of fMRI (GIFT) Matlab toolbox version 1.3c (http://icatb.sourceforge.net). ICA is a data-driven multivariate analysis method that identifies distinct groups of brain regions with the same temporal pattern of hemodynamic signal change. FMRI time series data for all participants were first compressed through principal component analysis (PCA). Three PCA data reduction stages reduce the impact of noise and make the estimation computationally tractable (Calhoun et al., 2001b; Calhoun et al., 2009b; Schmithorst and Holland, 2004). The final dimensionality of the data was estimated to be twenty maximally-independent components using the modified minimum description length (MDL) criteria tool built

into GIFT (Li et al., 2007). The data reduction was followed by a group spatial ICA, performed on the participants' aggregate data, resulting in the final estimation of our independent components. The algorithm used in this process was the infomax algorithm, which minimizes the mutual information of network outputs (Bell and Sejnowski, 1995).

From the group spatial ICA, we reconstructed spatial maps and their corresponding ICA time courses that represented both the spatial and temporal characteristics of each component, subject, and session. These characteristics are able to depict component and subject group variability existent in the data. In all, this resulted in 10,680 independent component spatial maps (267 subjects × 2 sessions × 20 independent components), each with an associated ICA time course of the data. These maps and time courses were then subjected to a second-level analysis to determine whether the resultant components were task-related or simply noise and/or artifacts. Components that are deemed as noise exhibit values that are randomly scattered throughout the brain or appear as rings on the edge of the brain (likely related to head motion) and are not plausibly caused by BOLD activity. For the remaining components, we report on only those components that were significant based on our planned comparison (e.g. task-related components exhibiting group differences).

*Statistical Analysis of Spatial Components*: We averaged the spatial maps produced during the spatial ICA across the two sessions. The spatial maps were then converted to z-score maps and then entered into a second level one-sample t-test to identify voxels which contributed significantly to a given component for all subjects, Next, these components were analyzed statistically and compared with group-specific

thresholds to observe regional brain activations and any potential trends among participant groups.

*Statistical Analysis of ICA Time Courses*: We performed a temporal sorting of the ICA time courses using an SPM5 design matrix containing one regressor corresponding to the auditory sensorimotor stimuli. Temporal sorting is a method by which we compare the model's time course with the ICA time course. Using a multiple linear regression sorting criteria, the concatenated ICA time courses were fit to the model time course. Upon completion of this step, components were then sorted according to the R-square statistic. This resulted in a set of beta weights for each regressor associated with a particular subject and independent component. The purpose of this temporal regression was to illustrate the significance of a particular component with respect to certain characteristics of the cognitive task that it represented. In other words, the value of the resulting beta weight directly indicated the degree to which the component was modulated by the task. From here, we calculated the event-related averages of the time courses for all components. Each plot of the event-related average depicts the level of task-related functional activity for that particular component over the course of the experimental period.

**Statistical Analyses**

For each independent component in this study, we performed a variety of analyses on the beta weights resulting from the ICA. These analyses included averages of the beta weights, one and two-sample t-tests, and correlations with symptoms and duration of illness for patients. The average beta values for regional task-modulation were calculated and sorted by subject group, by site as a whole, and by subject group for each site. The

one and two-sample t-tests were performed on the beta values obtained for each component to observe any possible significant differences in modulation within and among the various participant groups. One-sample t-tests provided information on the magnitude and direction of the modulation for each experimental group (schizophrenia patient groups and healthy controls) within particular brain regions, whereas the two-sample t-tests compared the differences in task modulation between the patient and control groups, as well as between the two patient groups based on duration of illness. The two-sample t-tests allowed us the opportunity to compare differences in the degree to which certain brain regions activated in response to this task.

The next step in the analysis of the fMRI data collected was to identify any potential correlations with positive and/or negative symptoms and with the duration of illness for all the schizophrenia patient groups. To complete this analysis, we conducted Pearson correlations of the beta weights with the positive and negative symptoms scores, as well as Spearman rank order correlations of the beta weights with the duration of illness in years. These comparisons were thresholded and corrected for multiple comparisons and between-group comparisons based on the false discovery rate (FDR).

**FNC Analysis**

Taking the five components that we considered to be of interest, we performed FNC analysis on these components to test for any possible temporal dependencies among them, as well as to explore the group differences between patients and control subjects. FNC analysis using the maximal lagged correlation method was performed on these five components using the FNC Matlab toolbox version 2.3beta

(http://mialab.mrn.org/software/index.php). These correlations were FDR corrected for multiple comparisons.

## RESULTS

### Behavioral Results

There were no significant differences found between schizophrenia patients and healthy controls in their response times to the auditory stimuli. Results showed that both patients and controls showed on average more than a 90% correct response to the auditory stimuli presented.

### Selected Independent Components

Twenty estimated independent components (ICs) were found. Of these, five ICs exhibited significant activation differences between patients and controls. These BOLD components overlapped very little with one another and were similar to those reported by others (Smith et al., 2009). The ICs and their respective component numbers are: a temporal lobe – left unilateral motor cortex IC (IC 18), a default mode IC (IC 8), a second default mode IC (IC 12), a right lateral frontoparietal lobe IC (IC 20), and a bilateral motor cortex IC (IC 11) (see Figure 4). A summary of the results observed is provided in the next section.

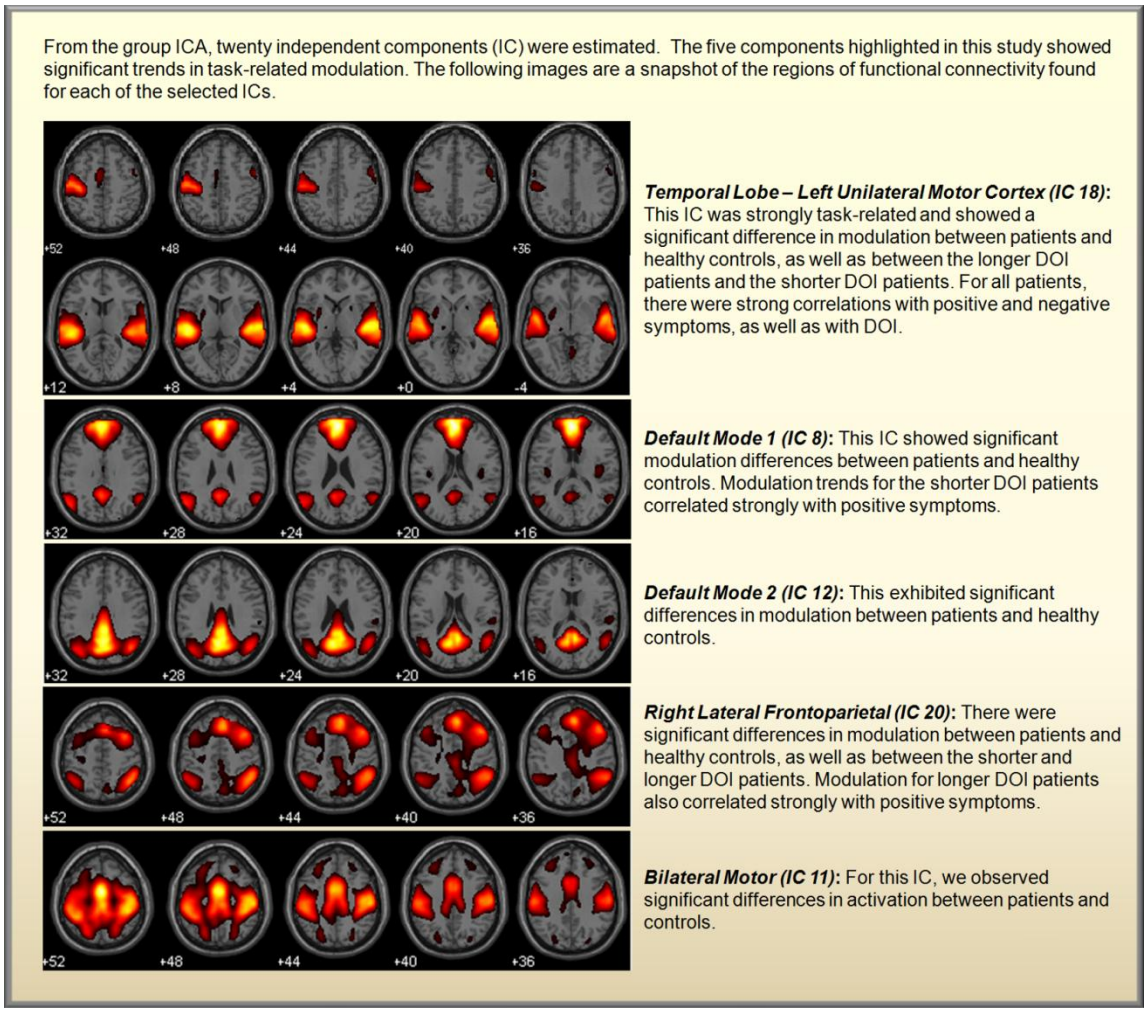


Figure 3: Regions of sensorimotor task-modulation

## Comparison of Task-related Time Courses

From the results of the statistical analysis of the beta weights shown in Table 2, we observed statistical trends toward increasingly positive or negative modulation as we progressed from the healthy control group, to the shorter DOI patient group, and finally to the longer DOI patient group. Details of these results are as follow.

*Temporal Lobe – Left Unilateral Motor Cortex (IC 18)*: This particular IC showed a combination of temporal lobe and left unilateral motor cortex activation, which was highly task-modulated. The patient group had significantly less positive modulation relative to the control group ($t_{165}$ = -1.88, $p < 0.05$). In addition, the patients with a longer

DOI had less positive modulation of this network relative to the patient group with the shorter DOI ($t_{120}$ = -2.28, $p < 0.05$).

*Default Mode 1 (IC 8)*: The anterior default mode network included the medial and superior frontal gyri, anterior cingulate gyrus, basal ganglia, and the precuneus. The patient group had significantly less negative modulation of this network relative to the control group ($t_{265}$ = 2.08, $p < 0.05$). We did not find any differences in the patient group in relation to DOI.

*Default Mode 2 (IC 12)*: The posterior default mode network included the posterior cingulate gyrus, preceneus, cuneus, and paracentral lobule. Like the anterior default mode, the patient group had significantly less negative modulation relative to the control group ($t_{265}$ = 2.75, $p < 0.05$). We did not find any differences in the patient groups in relation to DOI.

*Right Lateral Frontoparietal (IC 20)*: The patient group had significantly less positive modulation of this network compared to the healthy control group ($t_{265}$ = -3.77, $p < 0.05$). The patient group with the longer DOI had significantly less positive modulation relative to the shorter DOI patients ($t_{120}$ = -2.42, $p < 0.05$). The longer DOI patient group showed almost no positive modulation of this network.

*Bilateral Motor Cortex (IC 11)*: The healthy control group had very weak modulation of this network that appeared to correlate weakly with the experimental run. The patient group had significantly more positive modulation of this network than the healthy controls ($t_{265}$ = 5.39, $p < 0.05$). We did not find any differences in the patient groups in relation to DOI.

The ages of the patients were somewhat correlated with their duration of illness ($r$ = 0.32). To ensure the reliability of our results, we also ran our analysis covarying for age, and the results were consistent with the findings reported.

| | | ***Temporal Lobe - Unilateral Motor*** | ***Default Mode 1*** | ***Default Mode 2*** | ***Right Lateral Fronto-parietal*** | ***Bilateral Motor*** |
|---|---|---|---|---|---|---|
| | Component Number | ***18*** | ***8*** | ***12*** | ***20*** | ***11*** |
| **Two-sample T-tests (t-values)** | Patients vs. Controls | **-1.88** | **2.08** | **2.75** | **-3.77** | **5.39** |
| **Beta Values (by subject group)** | Healthy Controls | **1.34** | **-0.41** | **-0.70** | **0.28** | **-0.11** |
| | Shorter DOI Patients | 1.30 | -0.31 | -0.53 | 0.20 | 0.10 |
| | Longer DOI Patients | 1.11 | -0.26 | -0.47 | 0.03 | 0.20 |
| | All Patients | **1.20** | **-0.29** | **-0.50** | **0.12** | **0.15** |
| **Symptom Correlations (rho)** | All Patients / Positive | **0.22** | -0.11 | -0.13 | 0.14 | 0.02 |
| | All Patients / Negative | **0.22** | -0.04 | -0.08 | 0.07 | 0.03 |
| **Correlation with DOI (rho)** | All Patients | **-0.24** | 0.06 | 0.08 | -0.13 | 0.07 |

Table 2: Statistical results of sensorimotor data

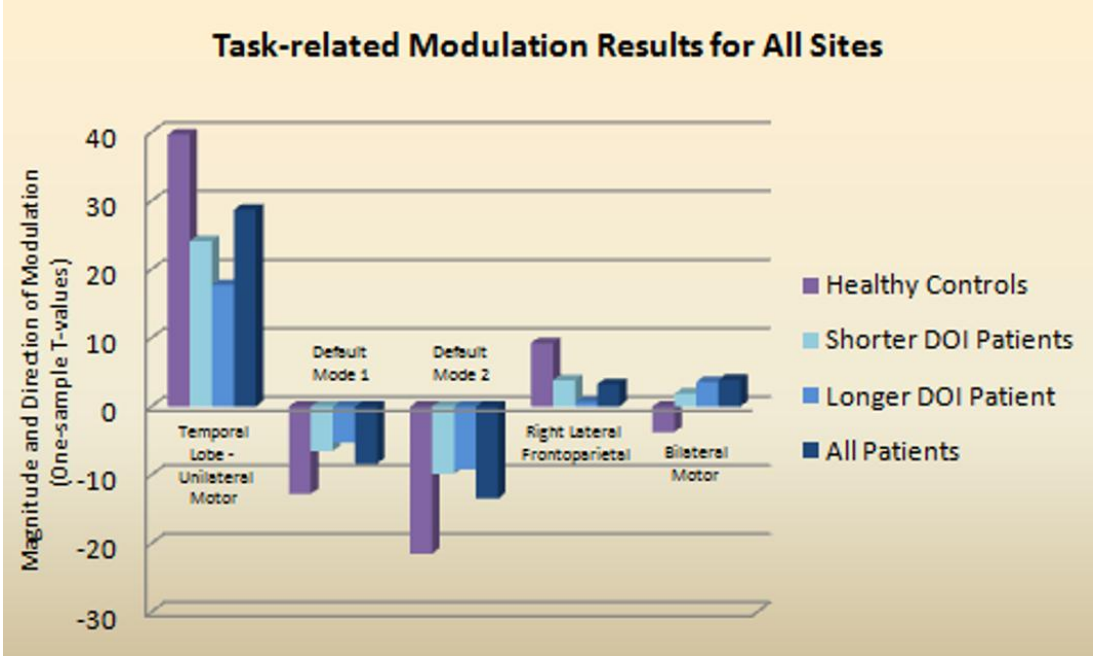


Figure 4: Task-related modulation results based on one-sample t-tests

**Correlations with Symptoms Scores and with Duration of Illness**

Correlations between task-modulated responses in the patient groups and the positive and negative symptom values and duration of illness in years were calculated and then thresholded at $p < 0.05$ (FDR corrected) using a nonparametric permutation approach. We found that activation for the temporal lobe-left unilateral motor IC correlated for the patient group with positive ($r = 0.22$, $p < 0.05$) and negative symptoms ($r = 0.22$, $p < 0.05$).

For the calculations of task-related connectivity with the DOI in the patient group, again, the temporal lobe-left unilateral motor IC showed significant results. We found a significant negative correlation with DOI for all patients ($r = -0.24$, $p < 0.05$). Detailed information on our findings is summarized in Table 2.

## Site Differences

To further verify the results derived in this investigation, we examined the effects separately for each of the four investigation sites (New Mexico, Iowa, Massachusetts, and Minnesota). By observing how the results from all the sites compared to one another, we were able to determine whether or not the modulations found for each of the significant independent components were similar to one another. We were encouraged to find similar trends in task modulation for all four sites. Averages of the one-sample t-test results were calculated by subject group and then by subject group for each site.

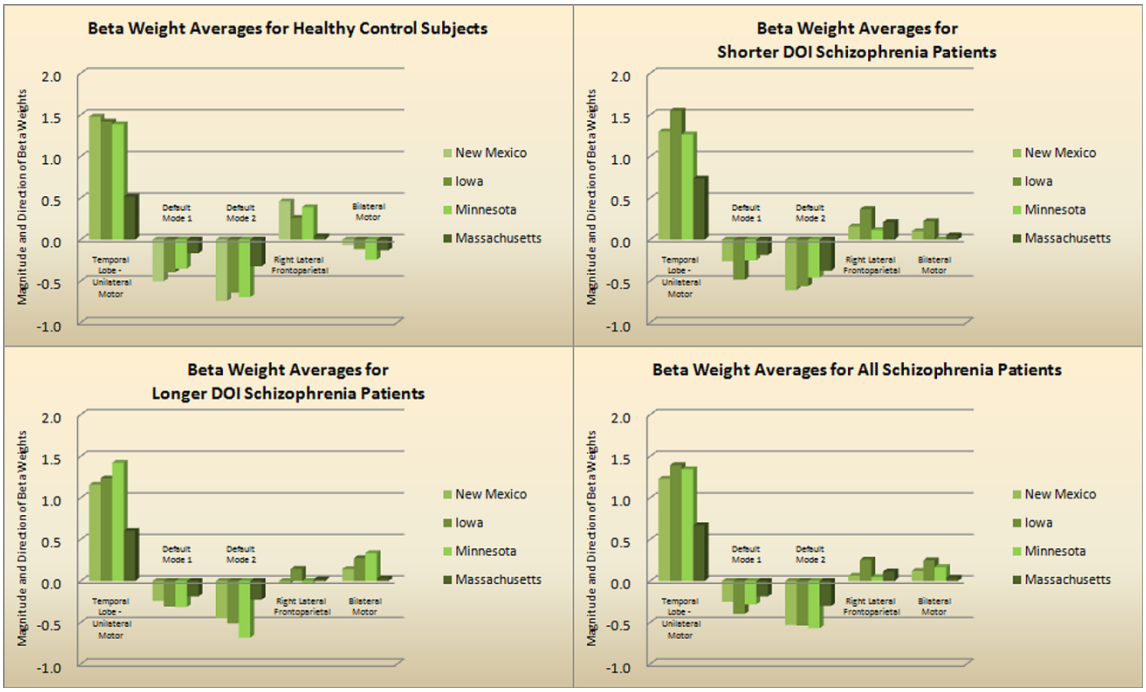


Figure 5: Average magnitude and direction of beta weights, differentiated by site, for all subject test groups

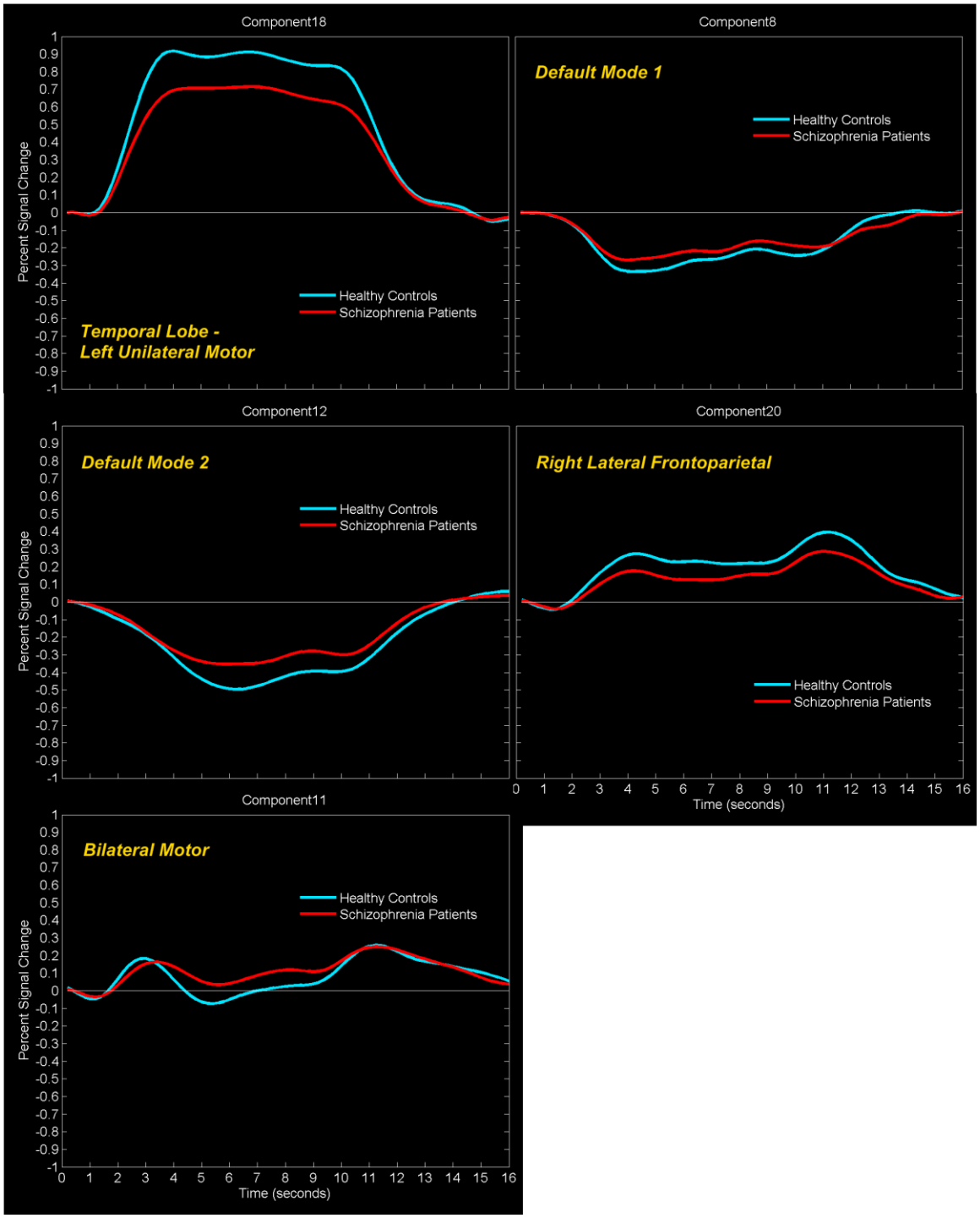


Figure 6: ICA time courses for all significant components

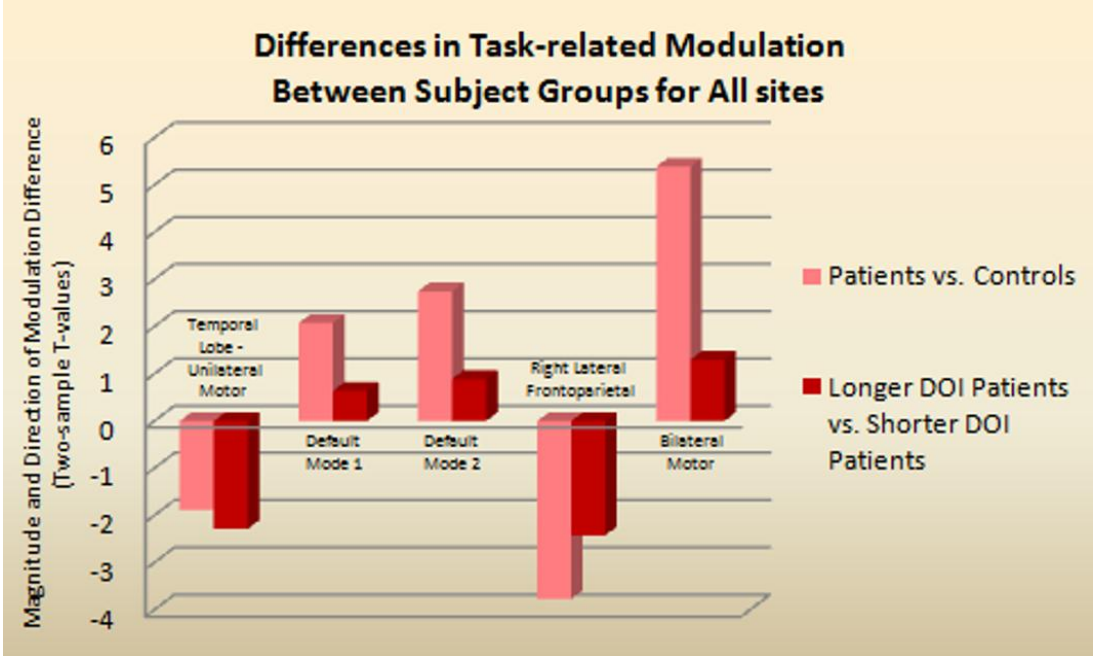


Figure 7: Differences in task-related modulation among the subject test groups based on two-sample t-tests

| Brain Regions | Brodmann Regions / Alternate Labels | *R/L (mm3)* | *R/L max t-values (MNI coordinates)* |
|---|---|---|---|
| ***Component 8 – Default Mode 1*** | | | |
| Medial Frontal Gyrus | 9, 10, 6, 8, 11, 25 | 32.4/32.3 | 42.8(-3,50,14)/42.5(3,56,14) |
| Superior Frontal Gyrus | 9, 10, 8, 6, 11 | 45.6/48.1 | 40.0(-3,54,22)/37.6(6,54,25) |
| Anterior Cingulate | 32, 24, 10, 33, 9, 25 | 12.9/13.4 | 39.4(-3,47,6)/42.2(3,47,6) |
| Basal Ganglia | 19, 37 / Corpus Callosum, Optic Tract, Red Nucleus, Dentate, Hypothalamus | 4.9/5.9 | 27.9(0,42,31)/14.2(42,22,-16) |
| Cingulate Gyrus | 31, 32, 24, 23 | 19.1/16.0 | 23.2(-3,36,29)/25.5(6,36,26) |
| Precuneus | 31, 7, 39, 23, 19 | 9.0/11.6 | 22.1(0,-54,33)/23.0(3,-51,33) |
| ***Component 11 – Bilateral Motor*** | | | |
| Medial Frontal Gyrus | 6, 32, 8, 10, 9, 11, 25 | 22.7/26.1 | 42.9(0,0,50)/37.8(3,-3,50) |
| Cingulate Gyrus | 24, 31, 32, 23, 9 | 20.6/20.7 | 40.6(0,-3,47)/38.6(3,-1,47) |
| Superior Frontal Gyrus | 6, 8, 9, 10, 11 | 41.3/45.1 | 34.6(0,5,49)/27.7(3,6,52) |
| Paracentral Lobule | 5, 6, 31, 4, 7 | 6.1/5.6 | 34.3(0,-9,47)/31.2(9,-44,60) |
| Precentral Gyrus | 4, 6, 3, 9, 44, 43, 13 | 30.2/26.7 | 34.1(-36,-26,57)/25.2(50,-19,37) |
| Postcentral Gyrus | 3, 5, 40, 2, 1, 7, 43 | 25.2/21.2 | 34.0(-39,-23,56)/33.0(27,-38,60) |
| ***Component 12 – Default Mode 2*** | | | |
| Cingulate Gyrus | 31, 23, 24, 32 | 20.5/15.1 | 42.1(-3,-39,38)/37.6(3,-36,40) |
| Precuneus | 7, 31, 23, 39, 19 | 32.6/31.8 | 38.9(-3,-39,43)/39.7(6,-60,28) |
| Posterior Cingulate | 31, 23, 30, 29, 18 | 8.2/9.4 | 35.5(-9,-54,19)/35.9(3,-60,25) |
| Cuneus | 7, 19, 18, 30, 17, 23 | 8.3/8.8 | 34.8(-6,-65,31)/36.0(3,-65,31) |
| Paracentral Lobule | 5, 31, 6, 4, 7 | 6.8/5.1 | 31.1(0,-41,49)/28.2(3,-38,49) |
| Sub-Gyral | 37, 7, 40, 2 / Hippocampus | 21.7/19.5 | 28.7(-12,-54,22)/28.3(12,-57,19) |
| ***Component 18 – Temporal Lobe / Left Unilateral Motor*** | | | |
| Superior Temporal Gyrus | 22, 13, 41, 21, 42, 38, 39 | 41.7/39.5 | 36.7(-48,-17,6)/38.9(48,-20,7) |
| Insula | 13, 40, 22, 41 | 12.2/14.5 | 33.2(-45,-17,4)/36.1(45,-17,6) |
| Transverse Temporal Gyrus | 41, 42 | 2.2/1.9 | 29.4(-48,-26,10)/37.2(48,-26,10) |
| Middle Temporal Gyrus | 21, 22, 38, 39, 19, 37, 20 | 27.0/27.0 | 25.7(-56,-6,-5)/20.6(65,-29,4) |
| Culmen | | 18.9/9.0 | 23.7(-18,-53,-15)/6.6(3,-67,-7) |
| Declive | | 14.9/14.5 | 22.7(-15,-56,-12)/10.5(27,-62,-17) |
| ***Component 20 – Right Lateral Frontoparietal*** | | | |
| Medial Frontal Gyrus | 8, 6, 9, 10, 32, 11, 25 | 25.2/25.8 | 29.4(-9,37,34)/22.1(3,28,43) |
| Superior Frontal Gyrus | 8, 6, 9, 10, 11 | 47.3/44.2 | 28.7(-6,31,43)/21.0(3,34,43) |
| Inferior Parietal Lobule | 40, 7, 39 | 19.5/17.4 | 27.6(-45,-50,49)/17.6(50,-47,44) |
| Middle Frontal Gyrus | 8, 9, 6, 46, 10, 11, 47 | 59.3/52.8 | 26.5(-45,28,29)/12.2(42,19,38) |
| Precentral Gyrus | 9, 6, 44 | 12.5/18.9 | 26.5(-45,22,35)/13.0(42,22,35) |
| Cingulate Gyrus | 32, 31, 24, 23 | 22.9/20.8 | 24.5(-3,36,29)/18.0(3,36,29) |

Table 3: Talairach coordinates for the group ICA

**FNC Analysis Results**

Significant correlations among time courses were detected for the primary components of interest, as shown in Figure 8. The direction and color saturation of the arrows indicate the direction and magnitude of the trend between a pair of components, such that for any two components *a* and *b*, $a \rightarrow b$ indicates that component *b* lags behind component *a* in its hemodynamic response by the number of seconds indicated by the color saturation of the arrow. The most significant pair-wise correlations are between the right lateral frontoparietal component and the temporal lobe-unilateral motor component within the healthy congrol group, as well as between the bilateral motor component and the temporal lobe-unilateral motor component in the patient group. There is a directional difference in the correlation between the bilateral motor and default mode 1 components. FNC analysis also revealed several significant differences in the time course correlations between the patient and healthy control groups.

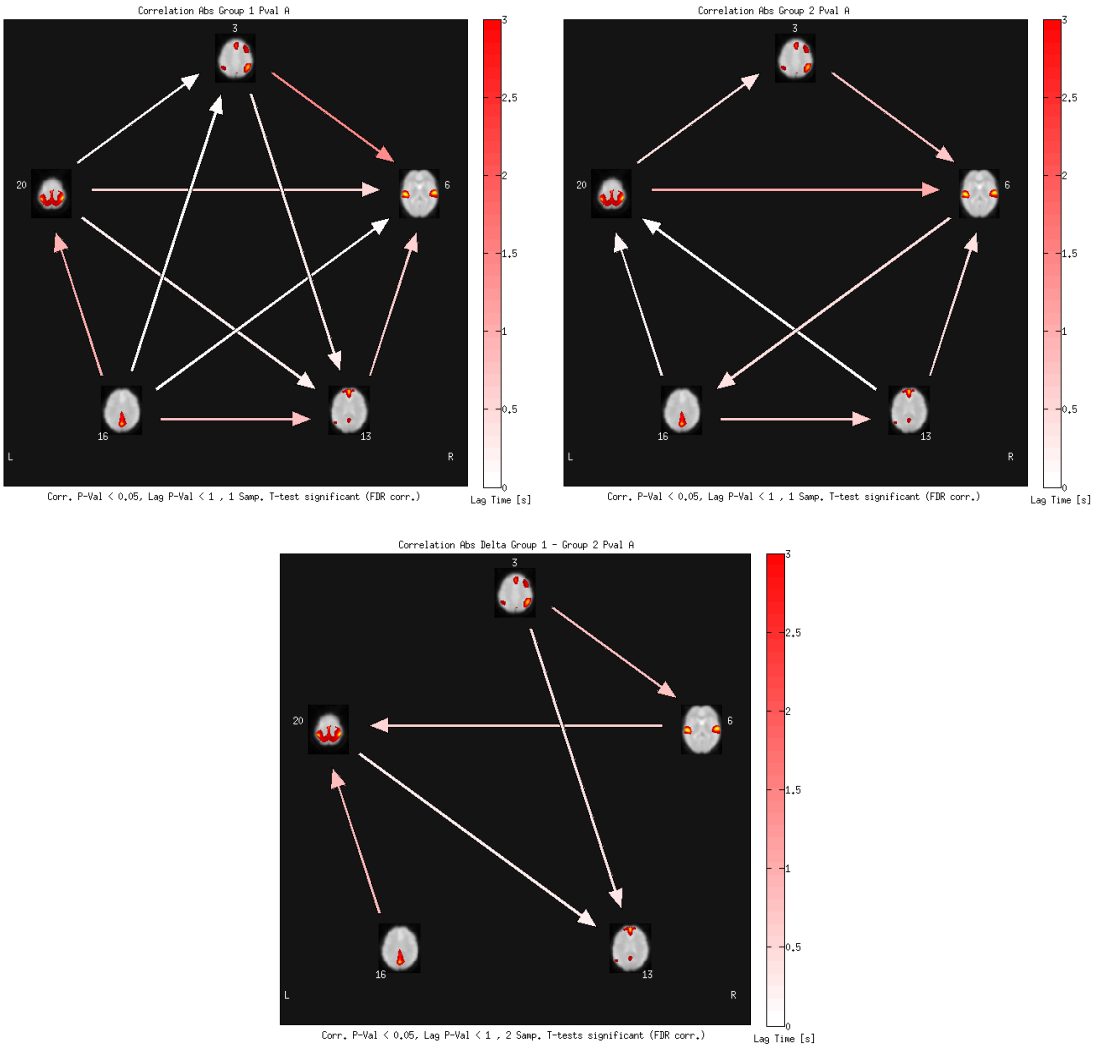


Figure 8: FNC results for healthy control subjects (top left), schizophrenia patients (top right), and the group differences detected between the two subject groups (HC – SZ) (bottom)

## DISCUSSION

The aim of this study was to compare group differences in functional connectivity between patients with schizophrenia and healthy controls, as well as to explore the functional network connectivity among the implicated regions of interest, using a basic sensorimotor task. The block-design paradigm implemented was used to stimulate auditory and sensorimotor regions. This task provided subjects with auditory stimuli, to which they responded with a motor reaction (button press). Using this simple design

paradigm, we were able to measure a robust response that was both auditory and motor in nature.

Consistent with our hypotheses, we found less positive modulation of temporal lobe-left unilateral motor and right lateral frontoparietal networks. We also found less negative modulation of both default mode networks in patients with schizophrenia relative to the healthy controls. The loss of positive modulation of the task related networks (temporal lobe-left unilateral motor and right lateral frontoparietal) and loss of negative modulation of the default mode networks in schizophrenia suggests that the diminished modulation of these networks may be relevant to the pathophysiology of schizophrenia.

Previous investigators have also demonstrated the loss of anticorrelation between the task related networks and default mode networks irrespective of task (working memory, target detection) and data analysis methods (ICA, region of interest approach) (Kim et al., 2009a; Kim et al., 2009b; Whitfield-Gabrieli et al., 2009). We have extended the findings by showing that the loss of positive modulation in task related networks (temporal lobe-left unilateral motor, right lateral frontoparietal) also occurs in a simple sensorimotor task that minimizes the effect of cognitive effort and motivation. In this block design, subjects are aware of the tone and subsequently allocate endogenous attention to sensory and perceptual filters (Cowan, 1995). The temporal lobe-left unilateral motor network includes the temporal cortex and insula, which represent the auditory cortex. Patients with schizophrenia have significantly less positive modulation of this network in this basic, sensory task. The decrease in positive modulation of this network suggests deficits in basic sensory processing of auditory stimuli. Furthermore,

this network correlates with both positive and negative symptoms. These results suggest that, within the patient group, increased modulation of this network is related to the severity of symptoms characteristic of schizophrenia.

Patients with schizophrenia also have a significant decrease in the right lateral frontoparietal network relative to the healthy controls. This reflects a deficit in patients with schizophrenia at the level of the upstream executive function used for endogenous attention (Cowan, 1995). This is also consistent with the repeated findings of dysfunction in the dorsolateral prefrontal cortex in schizophrenia (Goldman-Rakic, 1994; Honey and Fletcher, 2006). These results may be consistent with aberrant top-down processing of attentional networks in patients with schizophrenia during a basic sensorimotor task.

Consistent with our hypothesis, the patients with schizophrenia had significantly less negative modulation of the default mode networks relative to the healthy control group during the sensorimotor task. This finding is consistent with previous investigators' findings of diminished negative modulation of these networks in patients with schizophrenia during auditory oddball discrimination, as well as during a working memory task (Garrity et al., 2007; Kim et al., 2009a; Kim et al., 2009b). The deactivation of the default mode networks in our study may be related to the combined sensory and motor component that our task required. Modulation of this network also correlated with the positive symptoms with the shorter DOI group. These findings are consistent with previous investigators using a similar methodology. Garrity *et al.* found a correlation of the medial frontal, temporal and cingulated gyri of the default mode also correlating with the severity of positive symptoms (Garrity et al., 2007).

The patients with the longer DOI (average 18.1 years) have less positive modulation of the temporal lobe-left unilateral motor and right lateral-frontal parietal network than the patients with the shorter DOI (average 2.9 years). Additionally, we observed statistical trends toward increasingly positive or negative modulation across all components as we progress from the healthy control group to the shorter DOI patient group to the longer DOI patient group. These results are consistent with structural studies showing evidence of progressive volume loss over the course of the illness in schizophrenia. A meta-analysis on voxel-based morphometry revealed that the most consistent findings were deficits in the left superior temporal gyrus and the left medial temporal lobe (Honea et al., 2005). Both of these anatomic locations are located in the temporal lobe - left unilateral motor component. Our findings suggest that the changes after the onset of schizophrenia may be progressive and limited to specific networks and anatomic locations. We also note that the default mode networks did not show any evidence of progressive changes with DOI.

FNC analysis revealed significant temporal dependencies among the components of interest for both the patient and healthy control groups. Consistent with previous research, there appear to be several associations in the hemodynamic responses within the sensorimotor network in healthy controls that differ or do not appear within the patient group (Jafri et al., 2008). Additionally, there were several significant differences in the correlations of the time courses between the two subject groups. This may indicate widespread differences in the functional integration of these networks, which may be associated with a dysfunction within the sensorimotor network of schizophrenia patients.

Future analysis could include a correlation of these results with DOI to further investigate a possible association of these trends with the duration and severity of this illness.

It has been shown that patients who exhibit symptoms of more chronic auditory hallucinations have reduced functional connectivity within the temporo-parietal area of the brain (Vercammen et al.). Our investigation did not assess how auditory hallucinations may have affected the functional connectivity of the regions described. However, given the possibility of overlap in the brain regions implicated in our study with those related to auditory hallucinations, we suggest this as a topic of interest for further investigation. The possible effect of antipsychotic medications on this simple motor task limits the interpretation of our study. Previous investigators have found significant differences in the BOLD response between medicated and unmedicated schizophrenia subjects during a simple motor task (finger-tapping) (Muller et al., 2002a; Muller et al., 2002b). These results have also been extended to differences in the BOLD signal among patients taking different types of antipsychotics based on relative antagonism of the dopamine D2 receptor (Braus et al., 1999). These previous results suggest that patients with schizophrenia treated with antipsychotics have less positive modulation of cortical motor areas relative to controls. We did find differences in the temporal lobe – left unilateral motor cortex (less positive modulation) and the bilateral motor cortex (more positive modulation) between the patients with schizophrenia and the controls. Both of these motor components may be susceptible to the effect of antipsychotics. Comparisons of neuroleptic naïve patients with medicated patients are challenging but would be particularly informative.

Another limitation of our results includes the cross-sectional design. Previous functional connectivity studies on first episode patients have found no changes in functional connectivity or increased functional connectivity in certain networks relative to healthy controls (Lui et al., 2009; Whitfield-Gabrieli et al., 2009). The loss of functional connectivity later in the disease course in our study is consistent with these previous findings. Our study also included data from four sites, but we did not find any site-related differences. It is evident that the beta-value results from the Massachusetts site followed the same trend in task-modulated response as the other three sites. However, the magnitude of the responses from this site appeared to be significantly lower than that of the other sites. To verify the validity of our statistical results and the inclusion of the Massachusetts data in this investigation, we removed the Massachusetts data and repeated all statistical analyses using only data from the three remaining sites. We found no significant difference between the results with the Massachusetts data included compared to the results with that data removed. The modulation response trends and correlations that we observed after the removal of the Massachusetts data were not significantly different from the original statistical results. For this reason, we feel justified in the inclusion of the Massachusetts data in this study. We also recognize that we have not excluded the possibility of top-down abnormalities on sensory processing in patients with schizophrenia. Further research using effective connectivity is needed to delineate the relationship between sensory processing deficits, attention networks and the default mode networks in patients with schizophrenia.

The block design including both auditory and motor aspects has a limitation in that the responses elicited are intrinsically related to one another and cannot be separated.

As such, we are not able to distinguish whether there is only an auditory deficit, only a sensorimotor deficit, or both. However, it is likely the last, given that several prior studies show both auditory and motor activity differences in patients. We can however say that for this particular task we found robust differences between patients and controls. In future investigations, it would be germain to separate these two domains in a controlled experiment.

The large number of subjects tested in this study helped to identify population trends with greater sensitivity, as well as to draw more accurate conclusions from the data. The implications of these findings for the diagnosis (and possible treatment) of schizophrenia are of interest and suggest a sensory processing deficit in acoustic and attentional networks in schizophrenia. Future studies are needed to delineate the effect of antipsychotic drugs on motor networks in a simple sensorimotor task, as well as long-term effects of antipsychotics on changes in functional connectivity in motor networks.

# CHAPTER 4 – PSYCHOPATHY

## INTRODUCTION

Psychopathy is a psychological personality disorder that affects approximately 1% of the total population, but a significantly larger percentage of the prison population. It is characterized by chronic immoral impulses and antisocial behavior. This construct is theorized to originate from neurological dysfunction within the brain. This syndrome manifests itself through a variety of symptoms, from aggressive narcissism and lack of guilt and remorse to severe patterns of irresponsibility, juvenile delinquency, prolific substance abuse, and socially deviant lifestyles. Diagnosis is currently based upon a thorough review of these symptoms that meet a scaled, diagnostic threshold.

It is widely considered that the psychopathic personality disorder is ultimately untreatable and that those who suffer from this are unable to be rehabilitated into society. As such, those who commit crimes and are diagnosed as psychopathic are generally left untreated and are either institutionalized in psychiatric hospitals, or more often, detained in prison. Given the currently limited options for treatment, there is increasing research into the neurological causes and correlates of psychopathy. The symptoms that are exhibited in psychopathy may be associated with a disruption in the communication between brain regions, resulting in the diversity of symptoms that present. Advances in applied functional neuroimaging techniques have been shown to quantify regional brain connectivity (Calhoun et al., 2001a; McIntosh, 1999). Previous studies have suggested that individuals who exhibit psychopathy symptoms may differ from control populations (Calhoun et al., 2001b).

The application of group independent component analysis (ICA) to fMRI data has been used in order to identify spatially distinct and temporally coherent components of brain activity (McKeown et al., 2002) When applied in conjunction with a specific task, it provides a measure of both functional connectivity and task-relatedness. This allows for the identification of brain networks involving multiple brain regions, as well as the ability to test for which of these networks are affected by the psychological disorder under investigation (Calhoun et al., 2001a).

The ultimate purpose of this investigation was to document the manner in which functional networks are affected by psychopathy and how the hemodynamic responses occurring within these networks correlate with scored psychopathy symptoms. In addition, we intended to probe the possibility for the existence of temporal dependencies among the components detected through FNC analysis. Based on prior studies on psychopathy in prison inmates, our hypothesis was that we would find evidence of aberrant connectivity within the paralimbic brain network (Calhoun et al., 2001b). We also hypothesized differences in connectivity between inmates who have low PCL-R scores and those who scored high on the PCL-R scale.

We implemented group ICA and FNC analysis to study the imaging results of an auditory oddball task performed by a large group of prison inmates diagnosed as exhibiting psychopathic symptoms. We present results from a remote, mobile-site fMRI study involving 102 prison inmates with psychopathy symptoms, each of whom performed the same auditory oddball task.

## METHODS

### Participants

The primary goal of this investigation was the study of the neural mechanisms of psychopathy at various levels of psychosis. In all, the MRN study members collected blood oxygen level dependent (BOLD) fMRI data from a total of 102 prison inmates. Participants were recruited all recruited from New Mexico prison populations and scanned remotely at the prison site in the Mobile MRI Scanning Facility (http://www.mrn.org/mobile-mri-scanning-facility/index.php).

Participants underwent a clinical interview to determine their level of psychopathy. Diagnoses were based on the Hare Psychopathy Checklist-Revised (PCL-R), successor to the Hare Psychopathy Checklist first formulated in 1980 (Hare, 1991). The PCL-R is used as a psycho-diagnostic rating scale to diagnose and assess the type and degree of severity of psychopathy within an individual. This scale contains twenty items, each of which is scored on a three-point scale. These twenty items are divided into two groups or "factors," each factor being further subdivided into two "facets" each. The combination of the facet 1 and facet 2 scores will give the total factor 1 score, and the combination of the facet 3 and facet 4 scores will give the factor 2 scores. The sum of the factor 1 and factor 2 scores give the total PCL-R score for the subject. The PCL-R total score provides information on the severity of psychopathy within an individual. Those with a total PCL-R score of 30 or greater qualify for a diagnosis of psychopathy.

The individual factor scores are meant to provide insight on the manner in which a subject is psychopathic. Factor 1 scores correspond to characteristics of "aggressive narcissism," whereas factor 2 scores correspond to antisocial characteristics and

criminality associated with impulsive violence and socially deviant lifestyles. A complete listing of the twenty items and their breakdown in the PCL-R are given in Figure 9. Subjects are scored on these items based on specific criteria, such as from clinical file information and from an interview with a professional licensed to administer these tests. However, the quality of these tests and interviews is based solely upon the background information available for the subject and how honestly the subject responds during the clinical interview.

| **Factor 1: Personality "Aggressive narcissism"** | **Factor 2: Case history "Socially deviant lifestyle"** |
|---|---|
| ▪ Glibness/superficial charm<br>▪ Grandiose sense of self-worth<br>▪ Pathological lying<br>▪ Conning/manipulative<br>▪ Lack of remorse or guilt<br>▪ Shallow affect<br>▪ Callous/lack of empathy<br>▪ Failure to accept responsibility for own actions | ▪ Need for stimulation/proneness to boredom<br>▪ Parasitic lifestyle<br>▪ Poor behavioral control<br>▪ Promiscuous sexual behavior<br>▪ Lack of realistic, long-term goals<br>▪ Impulsivity<br>▪ Irresponsibility<br>▪ Juvenile delinquency<br>▪ Early behavior problems<br>▪ Revocation of conditional release |
| **Traits not correlated with either factor**<br>▪ Many short-term marital relationships<br>▪ Criminal versatility | |

Figure 9: PCL-R list items broken down by factor

Measures of the degree of severity of psychopathy symptoms were obtained using the PCL-R list. Participants ranged in age from 18 to 61 years of age, with an average age of 34.6 years and standard deviation of 10 year, and were generally untreated by medication. Any recruited subjects who were found unable to correctly perform the task

during practice were excluded from participating in the study. All subjects were completely fluent in English. A breakdown of the demographic and clinical data is provided in Table 4.

| | Age | Factor 1 | Factor 2 | Total Score |
|---|---|---|---|---|
| **Mean (all subjects)** | 34.6 | 6.7 | 12.7 | 21.5 |
| **Standard Deviation** | 10.0 | 3.4 | 4.1 | 7.1 |
| **Mean (PCL-R total score <= 20)** | 36.0 | 4.4 | 9.6 | 15.3 |
| **Standard Deviation** | 10.4 | 2.3 | 3.4 | 3.8 |
| **Mean (20 < PCL-R total score < 30)** | 33.7 | 7.4 | 14.6 | 24.4 |
| **Standard Deviation** | 10.0 | 2.4 | 2.2 | 2.5 |
| **Mean (PCL-R total score >= 30)** | 32.9 | 11.4 | 17.3 | 32.4 |
| **Standard Deviation** | 8.5 | 2.1 | 1.9 | 2.6 |

Table 4: Psychopathy demographics and PCL-R scores

**Task**

This task implemented a block design, auditory oddball paradigm in which the auditory stimuli were presented to each participant over the course of two runs while undergoing the fMRI scan. Wearing headphones to shield from the noise of the scanner, each participant was presented with a series of pseudorandom auditory stimuli (tones). Participants were asked to respond only to target stimuli by pressing a single button of the MIND input device (http://www.mrn.org/mind-input-device/index.php), while

ignoring (no button press) the standard tones and novel, computer-generated tones. During a test scan, the volume was calibrated to ensure that all test subjects were able to hear the tones comfortably over the background noise of the actual scanner. Consequently, the volume of the tones varied depending on the subject's degree of hearing during the audio setup for the task, therefore minimizing any auditory signal differences among groups with different hearing capabilities.

The auditory stimuli consisted of standard, target, and novel tones. In an auditory oddball paradigm, the standard stimuli are presented the most frequently, usually at a probability of about $p \approx 0.80$. The pitch of these standard stimuli is typically about 1 kHz. The target and novel stimuli are presented more infrequently, generally at a probability of $p \approx 0.10$ each. The target stimuli tones are presented at a different pitch from the standard tones, typically at about 1.2 kHz, whereas the novel stimuli are complex, computer generated sounds that vary in pitch during a single presentation. In all, these tones are presented in pseudorandom order, each tone lasting for about 200 ms. Because of the pseudorandom order in which they are presented, the interstimulus interval between tones will range from 500 – 2100 ms each time, depending on the paradigm design. In this study, there were a total two sessions per subject. There were multiple runs of the paradigm during each scanning session, each run consisting of the same number of stimuli (usually $\sim 100$). To ensure that hemodynamic responses were not induced by the type of stimuli presented, the target and novel presentation sequences were exchanged between runs in this study to balance their presentation. Prior to execution of the task in the scanner, all subjects practiced performing this task to ensure

capability in completing it correctly. Participants unable to perform the task correctly were excluded from the study.


Figure 10: Auditory oddball paradigm sample sequence - the three different stimuli are represented by different shapes and are unevenly-spaced to demonstrate the pseudorandom presentation

**Imaging Parameters**

Functional data were acquired at the remote site with EPI sequences on a Siemens 1.5 Tesla (T) MR scanner. The imaging sequence parameters are as follow: TR = 2000ms, TE = 29ms, FA = 65 degrees, FOV = 24x24cm, 64×64 matrix, 3.4 by 3.4mm in plane resolution, slice thickness = 5mm, 27 slices. This sequence covers the entire brain (150mm) in 1.5 seconds.

**Data Analysis**

*Preprocessing*: FMRI data were preprocessed using the SPM5 software package. Images were motion-corrected using INRIalign – an algorithm unbiased by local signal changes (Freire and Mangin, 2001; Freire et al., 2002). Data were spatially normalized into the standard Montreal Neurological Institute space (Friston, 1995) and slightly sub-sampled to 3×3×3 mm, resulting in 53×63×46 voxels. Next the data were spatially smoothed with a 10×10×10 mm full width at half-maximum Gaussian kernel. The resulting coordinates were converted to the Talairach and Tournoux standard space for anatomical mapping (Talairach and Tournoux, 1988).

**Independent Component Analysis**

Following the SPM5 preprocessing, a group ICA was performed on the preprocessed data (Calhoun et al., 2001b). The methods prescribed by these processes were organized in batch scripts and performed via the group ICA of fMRI (GIFT) Matlab

toolbox version 1.3c (http://icatb.sourceforge.net). FMRI time series data for all participants were first compressed through principal component analysis (PCA). There were three PCA data reduction stages which helped to reduce the impact of noise as well as to make the estimation computationally tractable (Calhoun et al., 2001b; Calhoun et al., 2009b; Schmithorst and Holland, 2004). The final dimensionality of the data from was estimated to be twenty-five maximally-independent components using the modified minimum description length (MDL) criteria tool built into GIFT (Li et al., 2007). The data reduction was followed by a group spatial ICA, performed on the participants' aggregate data, resulting in the final estimation of our independent components. The algorithm used in this process was the infomax algorithm, which attempts to minimize the mutual information of network outputs (Bell and Sejnowski, 1995).

From the group spatial ICA, we reconstructed spatial maps and their corresponding ICA time courses that represented both the spatial and temporal characteristics of each component, subject, and session. These characteristics are able to depict component and subject group variability existent in the data. In all, this resulted in 5100 independent component spatial maps (102 subjects × 2 sessions × 25 independent components), each with an associated ICA time course of the data. These maps and time courses were then subjected to a second-level analysis to determine whether the resultant components were task-related or simply noise and/or artifacts.

*Statistical Analysis of Spatial Components*: We averaged the spatial maps produced during the spatial ICA across the two sessions. The spatial maps were then converted to z-score maps and then entered into a second level one-sample t-test to identify voxels that contributed significantly to a given component for the group. Next,

these components were analyzed statistically and compared with group-specific thresholds to observe trends in task modulation among the subjects.

*Statistical Analysis of ICA Time Courses*: We performed a temporal sorting of the ICA time courses using an SPM5 design matrix containing three regressors corresponding to the three auditory oddball stimuli (standards, targets, and novels). Temporal sorting is a method by which we compare the model's time course with the ICA time course. Using a multiple linear regression sorting criteria, the concatenated ICA time courses were fit to the model time course. Upon completion of this step, components were then sorted according to the R-square statistic. This resulted in a set of beta weights for each regressor associated with a particular subject and independent component. The purpose of this temporal regression was to illustrate the significance of a particular component with respect to certain characteristics of the experiment that it represented. In other words, the value of the resulting beta weight directly indicated the degree to which the component was modulated by the task. From here, we calculated the event-related averages of the time courses for all components. Each plot of the event-related average depicts the level of task-related functional activity for that particular component over the course of the experimental period.

**Statistical Analyses**

For each independent component in this study, we performed a variety of analyses on the beta weights resulting from the ICA. These analyses included the mean and standard deviation of the beta weights, one and two-sample t-tests on the beta weights, spectral analyses of the time courses, and two sets of correlations – the first of the beta weights with PCL-R scores, and the second of the spectral analysis results with PCL-R

scores. We had initially intended on performing an analysis based solely on the comparison of the task-modulated differences between the set of subjects who scored "low" on the total PCL-R scale (PCL-R $\leq 20$) and the set of subjects who scored "high" on the total PCL-R scale (PCL-R $\geq 30$), using the correlations of the beta weights with the PCL-R scores to further support these results. However, because we were unable to find many significant differences between these groups with strong beta weight correlations with scores, we decided to include an analysis of the time course frequency spectra to see how those results correlated with the PCL-R scores.

The mean and standard deviation for task modulation of the hemodynamic response were calculated for the entire set of subjects and for the score-related subject subgroups. Next, one and two-sample t-tests were performed on the beta values obtained for each component to observe any possible significant differences in modulation within and among the various participant groups. The one-sample t-tests provided information on the degree and direction of the task modulation for each subject group within particular brain regions, whereas the two-sample t-tests compared the differences in modulation between the low PCL-R group (those subjects with a PCL-R score $\leq 20$) and the high PCL-R group (those subjects with a PCL-R score $\geq 30$. The two-sample t-tests allowed us the opportunity to compare differences in the degree to which certain brain regions exhibited a hemodynamic response to this task.

The next step in the analysis of the fMRI data collected was to identify any potential correlations between the beta weights and PCL-R scores for both group ICA results. To complete this analysis, we conducted Pearson correlations for the

aforementioned groups. These comparisons were thresholded and corrected for multiple comparisons based on the false discovery rate (FDR).

The final statistical analysis we performed was the spectral analysis of the time courses for all components. Spectral analysis employs the fast Fourier transform to estimate the component frequencies within a set of data. In this case, we estimated the frequencies based on the time courses for each of the components in this study. The resulting frequencies for each component in this analysis were output and separated into a set of six bins, which correspond to a histogram of the component's frequency spectra. Using these results, we then performed a correlation between these spectra and the series of PCL-R scores (factor 1, factor 2, and total).

**FNC Analysis**

Taking the components that we considered to be of interest, we performed FNC analysis on these components to test for any possible temporal dependencies among them, as well as to explore the group differences PCL-R subgroups. FNC analysis using the maximal lagged correlation method was performed on these components using the FNC Matlab toolbox version 2.3beta (http://mialab.mrn.org/software/index.php). These correlations were FDR corrected for multiple comparisons.

## RESULTS

We performed a full statistical analysis on the group ICA results. Twenty-five independent components (ICs) were estimated through group ICA. Of these, four ICs exhibited notable trends in modulation and/or significant correlations with PCL-R scores. The ICs and their respective component numbers are: a default mode component (10), a

parietal component (14), a second default mode component (21), and a visual component (24) (see Figure 3). Additionally, ten estimated ICs were found for the paralimbic ICA results. A summary of the results observed are provided in the next section.

**Comparison of Task-related Time Courses**

From group ICA, we revealed that modulation in the default mode 1 region (IC 10) was focused in the posterior, visual parietal brain region. We also discovered a second default mode (IC 21) that showed modulation focused in the anterior region of the brain. In addition to those ICs, the parietal (IC 14) and visual components (IC 24) showed task-related modulation trends that were deemed significant enough to continue with statistical analyses. However, only the visual component showed any significant differences between the low and high-scoring PCL-R subjects. Statistics on the one and two-sample t-test results on the beta weights are provided in the proceeding tables. Following these tables are figures illustrating the trends in modulation for the group ICA components of interest, along with their associated time courses.

| *T-tests* | **Default Mode 1** | **Parietal** | **Default Mode 2** | **Visual** |
|---|---|---|---|---|
| **Component Number** | **10** | **14** | **21** | **24** |
| ***One-sample T-test*** | | | | |
| **PCLR <= 20** | | | | |
| ***Standard*** | -3.50 | -9.45 | -4.85 | -4.32 |
| ***Target*** | -3.85 | 5.52 | **-9.25** | 5.41 |
| ***Novel*** | -5.50 | -3.56 | -6.51 | 1.13 |
| **20 < PCLR <30** | | | | |
| ***Standard*** | -5.12 | -9.41 | -3.02 | -4.70 |
| ***Target*** | -5.90 | 1.70 | **-8.14** | 1.52 |
| ***Novel*** | -6.54 | -3.85 | -7.94 | -1.20 |
| **PCLR >= 30** | | | | |
| ***Standard*** | -0.62 | -7.19 | -2.63 | -2.38 |
| ***Target*** | -0.67 | 1.80 | **-4.61** | 0.85 |
| ***Novel*** | -2.22 | -3.96 | -3.30 | -0.82 |
| ***Two-sample T-test*** | | | | |
| **PCLR low vs. high** | | | | |
| ***Standard*** | -1.40 | 0.08 | 0.21 | -0.24 |
| ***Target*** | -1.18 | 1.46 | -1.07 | 1.99 |
| ***Novel*** | -0.52 | 1.24 | 0.32 | 1.37 |

Table 5: Results from the one and two-sample t-tests performed on the beta weights, broken down by PCL-R subject group

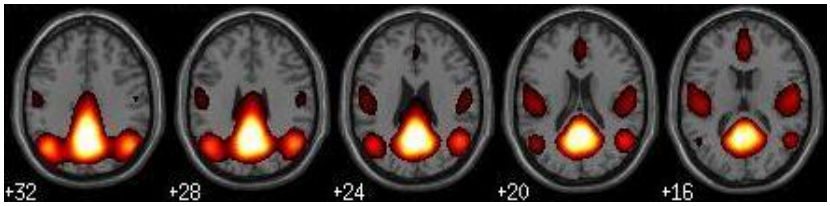


Default Mode 1 (IC 10)

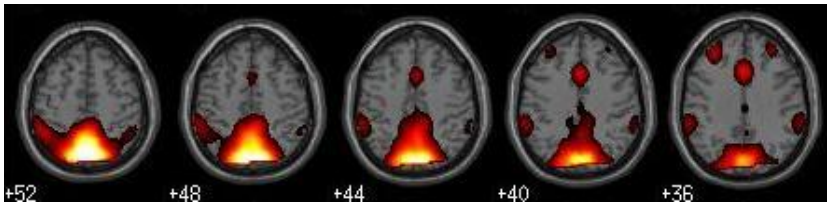


Parietal (IC 14)

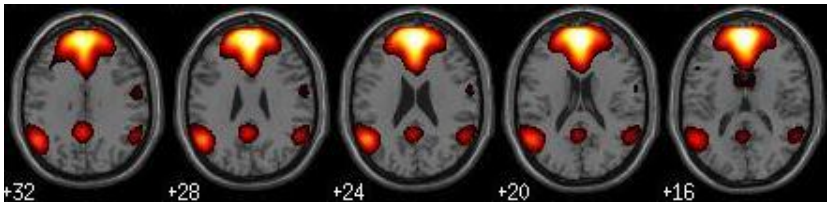


Default Mode 2 (IC 21)

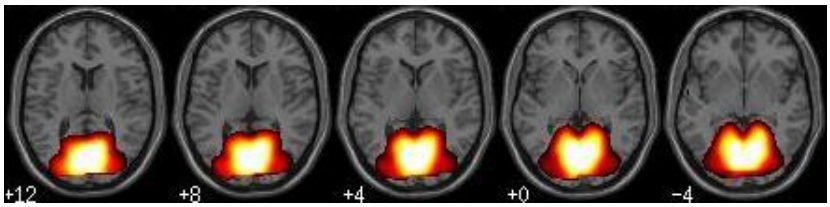


Visual (IC 24)

Figure 11: Regions of auditory oddball task-modulation

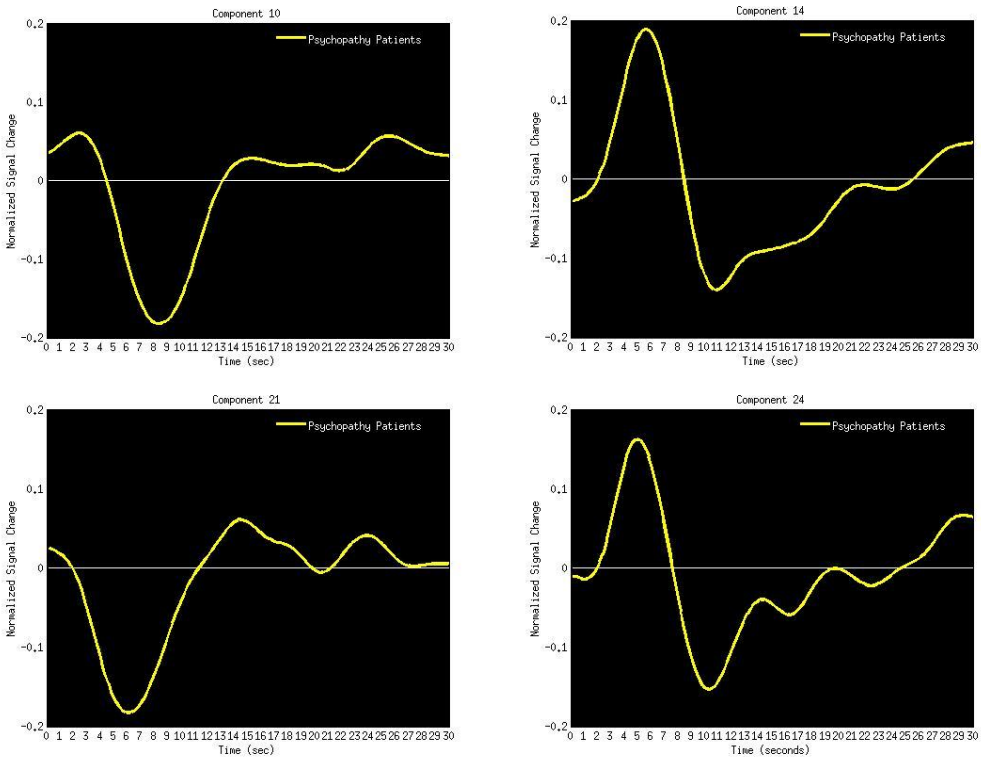


Figure 12: Associated time courses for the significant components

## Correlations with PCL-R Scores

In addition to the standard t-tests, we calculated correlations of the beta weights with the factor 1, factor 2, and total PCL-R scores to see if we could find any significant correlations with any of the PCL-R symptom factors and/or overall total PCL-R symptoms. From statistics calculated for the group ICA beta weight results, we found significant, negative correlations of the parietal and visual component beta weights with the total PCL-R scores. Additionally, we show significant correlations of the beta weights across all the components for the high-scoring PCL-R group with the factor 2 scores. Results of the correlations with factor 1, factor 2, and total PCL-R scores are given in the proceeding tables.

| *Correlations with PCL-R Total Scores* | Default Mode 1 | Parietal | Default Mode 2 | Visual |
|---|---|---|---|---|
| **Component Number** | **10** | **14** | **21** | **24** |
| ***Correlations: PCLR <= 20*** | | | | |
| ***Standard*** | 0.07 | -0.04 | 0.11 | -0.05 |
| ***Target*** | 0.15 | -0.11 | 0.10 | 0.03 |
| ***Novel*** | -0.07 | -0.13 | 0.16 | -0.32 |
| ***Correlations: 20 < PCLR < 30*** | | | | |
| ***Standard*** | -0.11 | -0.23 | -0.12 | -0.19 |
| ***Target*** | 0.31 | 0.17 | -0.16 | -0.13 |
| ***Novel*** | -0.11 | -0.25 | -0.10 | -0.15 |
| ***Correlations: PCLR >= 30*** | | | | |
| ***Standard*** | -0.16 | -0.39 | -0.28 | -0.19 |
| ***Target*** | 0.13 | -0.11 | -0.19 | 0.12 |
| ***Novel*** | 0.22 | -0.09 | -0.04 | -0.28 |
| ***Correlations: All Subjects*** | | | | |
| ***Standard*** | 0.01 | -0.16 | -0.07 | -0.20 |
| ***Target*** | 0.14 | -0.21 | 0.12 | -0.20 |
| ***Novel*** | 0.01 | -0.10 | 0.01 | -0.13 |

Table 6: Correlations of the beta weights with PCL-R total scores for the normal ICA

| *Correlations with Factor 1 Scores* | Default Mode 1 | Parietal | Default Mode 2 | Visual |
|---|---|---|---|---|
| **Component Number** | **10** | **14** | **21** | **24** |
| ***Correlations: PCLR <= 20*** | | | | |
| ***Standard*** | -0.01 | -0.18 | -0.19 | -0.07 |
| ***Target*** | 0.05 | -0.30 | 0.02 | 0.16 |
| ***Novel*** | -0.28 | -0.14 | -0.04 | 0.00 |
| ***Correlations: 20 < PCLR < 30*** | | | | |
| ***Standard*** | -0.19 | -0.08 | -0.07 | -0.24 |
| ***Target*** | -0.04 | -0.23 | 0.02 | -0.14 |
| ***Novel*** | 0.05 | -0.10 | -0.15 | -0.15 |
| ***Correlations: PCLR >= 30*** | | | | |
| ***Target*** | 0.10 | -0.45 | 0.54 | -0.10 |
| ***Standard*** | -0.11 | -0.18 | -0.19 | -0.13 |
| ***Novel*** | 0.25 | -0.09 | 0.06 | -0.12 |
| ***Correlations: All Subjects*** | | | | |
| ***Standard*** | -0.18 | -0.08 | -0.16 | -0.25 |
| ***Target*** | -0.05 | -0.25 | -0.07 | -0.08 |
| ***Novel*** | -0.08 | -0.02 | -0.11 | -0.06 |

Table 7: Correlations of the beta weights with PCL-R factor 1 scores

| *Correlations with Factor 2 Scores* | Default Mode 1 | Parietal | Default Mode 2 | Visual |
|---|---|---|---|---|
| **Component Number** | **10** | **14** | **21** | **24** |
| ***Correlations: PCLR <= 20*** | | | | |
| ***Standard*** | -0.07 | 0.11 | 0.19 | -0.08 |
| ***Target*** | -0.16 | 0.22 | 0.21 | -0.08 |
| ***Novel*** | -0.26 | 0.08 | -0.17 | 0.16 |
| ***Correlations: 20 < PCLR < 30*** | | | | |
| ***Standard*** | 0.00 | 0.26 | 0.08 | 0.14 |
| ***Target*** | -0.16 | 0.16 | -0.10 | 0.10 |
| ***Novel*** | -0.06 | 0.27 | 0.09 | 0.09 |
| ***Correlations: PCLR >= 30*** | | | | |
| ***Standard*** | -0.22 | 0.28 | -0.45 | -0.01 |
| ***Target*** | 0.26 | -0.07 | -0.01 | 0.53 |
| ***Novel*** | -0.23 | 0.49 | -0.24 | 0.25 |
| ***Correlations: All Subjects*** | | | | |
| ***Standard*** | -0.11 | 0.10 | 0.00 | -0.13 |
| ***Target*** | -0.12 | 0.03 | -0.04 | -0.08 |
| ***Novel*** | -0.16 | 0.16 | -0.10 | 0.10 |

Table 8: Correlations of the beta weights with PCL-R factor 2 scores

**Analysis of Frequency Spectra**

To supplement the correlation results of the beta weights with the PCL-R scores, we calculated the frequency spectra of the time courses for all the components. The output of this spectral analysis is a histogram of all the components' spectra, with six bins per component. We correlated this output with the PCL-R series of scores to get an idea of how the time course frequencies correlated with those scores. We found that the time course frequency spectra for the default mode 2 component correlated the strongest with all these scores, with the default mode 1 component not too far behind. The results of these correlations are displayed in the following table.

| *Correlations for Spectral Frequencies with PCL-R Scores* | Default Mode 1 | Parietal | Default Mode 2 | Visual |
|---|---|---|---|---|
| **Component Number** | **10** | **14** | **21** | **24** |
| ***Factor 1*** | 0.70 | 0.50 | 0.88 | 0.45 |
| ***Factor 2*** | 0.61 | 0.62 | 0.97 | 0.53 |
| ***Total Scores*** | 0.69 | 0.55 | 0.93 | 0.46 |

Table 9: Correlations of the time course frequency spectra with the factor 1, factor 2, and total PCL-R scores

**FNC Analysis Results**

FNC analysis revealed several significant associations among the component time courses, as shown in Figure 14. Within both the low and high PCL-R subgroups we detected significant correlations among the time courses for all the components. However, the significance in the association between the visual component and the anterior default mode component disappears in the high PCL-R group. Analysis also revealed a difference between the two subgroups in the direction of the correlational association between the visual component and the posterior default mode component. No significant differences between the low PCL-R subjects and the high PCL-R subjects were detected.

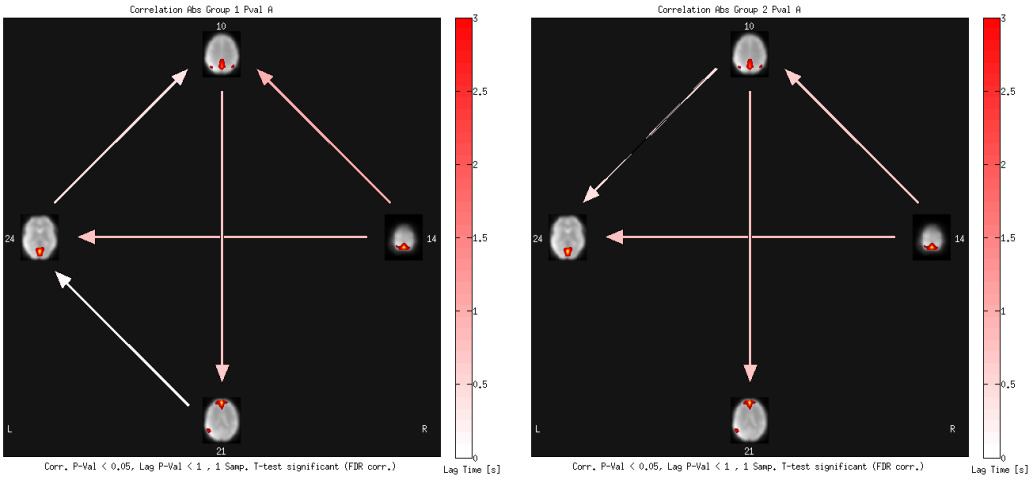


Figure 13: FNC results for low PCL-R subjects (left) and high PCL-R subjects (right)

## DISCUSSION

Based on the results of these analyses, we found that group ICA was able to successfully detect trends of task-related modulation induced by the auditory oddball task in psychopathy subjects. Of particular significance were the results of the two-sample t-test within the visual component for the target stimulus presentation, as well as the correlations of the beta weights with the PCL-R total scores for the parietal and visual components. Additionally, we found significant correlations for the beta weights of the high-PCL-R scoring subjects with the factor 2 scores across all the components. Because factor 2 has the more severe, criminal characteristics of the total PCL-R list, this may indicate a relationship between aberrant modulation within these regions and criminal behavior.

To further supplement and support this information, we continued to perform an analysis on the frequency spectra of the time courses for the significant components

indicated. The results of these correlations showed relatively high significance. This investigation is still in the process of interpretation of the statistical results.

We were successful in detecting significant correlations among the time courses of the components of interest for both the low and high PCL-R subject groups. The disappearance of the significance in the association in modulation between the visual and anterior default mode components in the high PCL-R subjects may indicate a dysfunction in the functional integration of those networks in psychopathy subjects. The difference in the direction of the correlation between the visual component and the posterior default mode component may also indicate a functional network difference between healthy populations and psychopathy subjects. We were unable to detect group differences between low-scoring and high-scoring PCL-R subjects in the temporal dependencies among the implicated components. This may have been caused by a variety of factors, including the task design paradigm used during the scan. However, the methods implemented in this study show a potential for the successful analysis of fMRI data collected from psychopathy subjects, upon which concrete and viable results may be discovered.

# CHAPTER 5 – CONCLUSION AND FUTURE WORK

## CONCLUSION

In this thesis, we described the widespread problem of mental disorders and the necessity for innovative medical imaging techniques to deconstruct the possible neural correlates involved in those disorders. We posed the fMRI image analysis methods of group ICA and FNC analysis as novel and efficient methods of investigating the functional connectivity and functional network connectivity of brain networks implicated in various psychopathologies.

We implemented these image analysis techniques on two large-scale and distinct psychopathology studies (schizophrenia and psychopathy) to demonstrate the capabilities of each method in not only detecting several, distinct task-modulated networks exhibiting a significant hemodynamic response to very different tasks, but also in revealing potential temporal dependencies among those network components. FNC analysis revealed significant dependencies in the temporal relationships among distinct brain regions for both the schizophrenia and psychopathy studies, as well as group differences between patient and control groups in the schizophrenia study. A major advantage to the implementation of group ICA and FNC analysis together is that FNC analysis does not require any additional or extraneous brain imaging data collection other than what has already been collected. This technique is merely an additional analysis step that simply takes the components estimated through group ICA as its input. FNC analysis is the next logical step in solidifying the versatility and usefulness of group ICA in both functional connectivity and functional network connectivity research. Used together, these image analysis methods provide an additional dimension of knowledge on the functional

mechanisms of the brain, with the potential to reveal deficits in the functional networks of those afflicted by a mental disorder. It has practicality and general applicability in the fields of functional connectivity and functional network connectivity.

## FUTURE RESEARCH TOPICS

Though group ICA has been implemented extensively in the field of functional connectivity with very solid and consistent results, the field of functional network connectivity is still relatively new and widely unexplored. This thesis focused on the method of FNC analysis that calculated the maximal lagged correlation between pair-wise combinations of components and provided information on the latency differences between those networks. However, this method is merely a look at the correlational trends between network activations and does not necessarily imply hemodynamic causation among the components being compared. Other methods of FNC analysis, such as Granger causality, are currently being developed and investigated to address the issue of causality in the hemodynamic responses among networks. Future development of this method of FNC analysis, along with other as yet undiscovered algorithms, is vital in the future FNC analysis as a reliable, analytical technique for the detection of causal relationships among the functional networks within the brain.

## REFERENCES

2000. Cross-national comparisons of the prevalences and correlates of mental disorders. WHO International Consortium in Psychiatric Epidemiology. Bull World Health Organ 78, 413-426.

Andreasen, N.C., 1983. The Scale for the Assessment of Negative Symptoms (SANS). The University of Iowa, Iowa City, IA.

Andreasen, N.C., 1984. The Scale for the Assessment of Positive Symptoms (SAPS). The University of Iowa, Iowa City, IA.

Andreasen, N.C., Flaum, M., Arndt, S., 1992. The Comprehensive Assessment of Symptoms and History (CASH). An instrument for assessing diagnosis and psychopathology. Arch Gen Psychiatry 49, 615-623.

Bell, A.J., Sejnowski, T.J., 1995. An information maximisation approach to blind separation and blind deconvolution. Neural Comput. 7, 1129-1159.

Biswal, B., Yetkin, F.Z., Haughton, V.M., Hyde, J.S., 1995. Functional connectivity in the motor cortex of resting human brain using echo-planar MRI. Magn.Res.Med. 34, 537-541.

Biswal, B.B., Van Kylen, J., Hyde, J.S., 1997. Simultaneous assessment of flow and BOLD signals in resting-state functional connectivity maps. NMR Biomed. 10, 165-170.

Braff, D.L., Saccuzzo, D.P., 1981. Information processing dysfunction in paranoid schizophrenia: a two-factor deficit. Am J Psychiatry 138, 1051-1056.

Braus, D.F., Ende, G., Weber-Fahr, W., Sartorius, A., Krier, A., Hubrich-Ungureanu, P., Ruf, M., Stuck, S., Henn, F.A., 1999. Antipsychotic drug effects on motor activation measured by functional magnetic resonance imaging in schizophrenic patients. Schizophr Res 39, 19-29.

Calhoun, V.D., Adali, T., 2006. 'Unmixing' Functional Magnetic Resonance Imaging with Independent Component Analysis. IEEE Eng.in Medicine and Biology 25, 79-90.

Calhoun, V.D., Adali, T., McGinty, V., Pekar, J.J., Watson, T., Pearlson, G.D., 2001a. fMRI Activation In A Visual-Perception Task: Network Of Areas Detected Using The

General Linear Model And Independent Component Analysis. NeuroImage 14, 1080-1088.

Calhoun, V.D., Adali, T., Pearlson, G.D., Pekar, J.J., 2001b. A Method for Making Group Inferences from Functional MRI Data Using Independent Component Analysis. Hum.Brain Map. 14, 140-151.

Calhoun, V.D., Adali, T., Pearlson, G.D., Pekar, J.J., 2001c. Spatial and temporal independent component analysis of functional MRI data containing a pair of task-related waveforms. Hum.Brain Map. 13, 43-53.

Calhoun, V.D., Adali, T., Pekar, J.J., Pearlson, G.D., 2003. Latency (in)sensitive ICA: Group Independent Component Analysis of fMRI Data in the Temporal Frequency Domain. NeuroImage 20, 1661-1669.

Calhoun, V.D., Eichele, T., Pearlson, G., 2009a. Functional brain networks in schizophrenia: a review. Front Hum Neurosci 3, 17.

Calhoun, V.D., Liu, J., Adali, T., 2009b. A Review of Group ICA for fMRI Data and ICA for Joint Inference of Imaging, Genetic, and ERP Data. NeuroImage 45, 163-172.

Cordes, D., Haughton, V., Carew, J.D., Arfanakis, K., Maravilla, K., 2002. Hierarchical clustering to measure connectivity in fMRI resting-state data. Magn Reson Imaging 20, 305-317.

Cordes, D., Haughton, V.M., Arfanakis, K., Carew, J.D., Turski, P.A., Moritz, C.H., Quigley, M.A., Meyerand, M.E., 2001. Frequencies contributing to functional connectivity in the cerebral cortex in "resting-state" data. AJNR Am.J.Neuroradiol. 22, 1326-1333.

Cordes, D., Haughton, V.M., Arfanakis, K., Wendt, G.J., Turski, P.A., Moritz, C.H., Quigley, M.A., Meyerand, M.E., 2000. Mapping functionally related regions of brain with functional connectivity MR imaging. AJNR Am.J.Neuroradiol. 21, 1636-1644.

Cowan, N., 1995. Attention and Memory: An Integrated Framework. Oxford Universtity Press, New York.

First, M., Spitzer, R.L., Gibbon, M., Williams, J.B., 1997. Structured Clinical Interview for DSM-IV-TR Axis I Disorders. American Psychiatric Press, Inc., Washington, D.C.

Ford, J.M., Mathalon, D.H., 2008. Neural synchrony in schizophrenia. Schizophr Bull 34, 904-906.

Freire, L., Mangin, J.F., 2001. Motion correction algorithms may create spurious brain activations in the absence of subject motion. NeuroImage 14, 709-722.

Freire, L., Roche, A., Mangin, J.F., 2002. What is the best similarity measure for motion correction in fMRI time series? IEEE Trans.Med.Imaging 21, 470-484.

Friedman, L., Stern, H., Brown, G.G., Mathalon, D.H., Turner, J., Glover, G.H., Gollub, R.L., Lauriello, J., Lim, K.O., Cannon, T., Greve, D.N., Bockholt, H.J., Belger, A., Mueller, B., Doty, M.J., He, J., Wells, W., Smyth, P., Pieper, S., Kim, S., Kubicki, M., Vangel, M., Potkin, S.G., 2008. Test-retest and between-site reliability in a multicenter fMRI study. Hum Brain Mapp 29, 958-972.

Friston, K., 1994. Functional and effective connectivity in neuroimaging: A synthesis. Hum Brain Mapp, 56-79.

Friston, K., 1995. Spatial Normalisation: A new approach.

Friston, K.J., Frith, C.D., 1995. Schizophrenia: a disconnection syndrome? Clin Neurosci 3, 89-97.

Garrity, A.G., Pearlson, G.D., McKiernan, K., Lloyd, D., Kiehl, K.A., Calhoun, V.D., 2007. Aberrant "default mode" functional connectivity in schizophrenia. Am J Psychiatry 164, 450-457.

Goldman-Rakic, P.S., 1994. Working memory dysfunction in schizophrenia. J Neuropsychiatry Clin Neurosci 6, 348-357.

Green, M.F., Kern, R.S., Braff, D.L., Mintz, J., 2000. Neurocognitive deficits and functional outcome in schizophrenia: are we measuring the "right stuff"? Schizophr Bull 26, 119-136.

Hare, R.D., 1991. Manual for the Hare Psychopathy Checklist-Revised. Multi-Health Systems, Toronto.

Holzman, P.S., Proctor, L.R., Levy, D.L., Yasillo, N.J., Meltzer, H.Y., Hurt, S.W., 1974. Eye-tracking dysfunctions in schizophrenic patients and their relatives. Arch Gen Psychiatry 31, 143-151.

Honea, R., Crow, T.J., Passingham, D., Mackay, C.E., 2005. Regional deficits in brain volume in schizophrenia: a meta-analysis of voxel-based morphometry studies. Am J Psychiatry 162, 2233-2245.

Honey, G.D., Fletcher, P.C., 2006. Investigating principles of human brain function underlying working memory: what insights from schizophrenia? Neuroscience 139, 59-71.

Jafri, M.J., Pearlson, G.D., Stevens, M., Calhoun, V.D., 2008. A method for functional network connectivity among spatially independent resting-state components in schizophrenia. NeuroImage 39, 1666-1681.

Javitt, D.C., 2009. When doors of perception close: bottom-up models of disrupted cognition in schizophrenia. Annu Rev Clin Psychol 5, 249-275.

Kessler, R.C., Berglund, P., Demler, O., Jin, R., Merikangas, K.R., Walters, E.E., 2005. Lifetime prevalence and age-of-onset distributions of DSM-IV disorders in the National Comorbidity Survey Replication. Arch Gen Psychiatry 62, 593-602.

Kim, D.I., Manoach, D.S., Mathalon, D.H., Turner, J.A., Mannell, M., Brown, G.G., Ford, J.M., Gollub, R.L., White, T., Wible, C., Belger, A., Bockholt, H.J., Clark, V.P., Lauriello, J., O'Leary, D., Mueller, B.A., Lim, K.O., Andreasen, N., Potkin, S.G., Calhoun, V.D., 2009a. Dysregulation of working memory and default-mode networks in schizophrenia using independent component analysis, an fBIRN and MCIC study. Hum Brain Mapp.

Kim, D.I., Mathalon, D.H., Ford, J.M., Mannell, M., Turner, J.A., Brown, G.G., Belger, A., Gollub, R., Lauriello, J., Wible, C., O'Leary, D., Lim, K., Toga, A., Potkin, S.G., Birn, F., Calhoun, V.D., 2009b. Auditory oddball deficits in schizophrenia: an independent component analysis of the fMRI multisite function BIRN study. Schizophr Bull 35, 67-81.

Li, Y., Adali, T., Calhoun, V.D., 2007. Estimating the number of independent components for fMRI data. Hum.Brain Map. 28, 1251-1266.

Lowe, M.J., Mock, B.J., Sorenson, J.A., 1998. Functional connectivity in single and multislice echoplanar imaging using resting-state fluctuations. NeuroImage 7, 119-132.

Lui, S., Deng, W., Huang, X., Jiang, L., Ma, X., Chen, H., Zhang, T., Li, X., Li, D., Zou, L., Tang, H., Zhou, X.J., Mechelli, A., Collier, D.A., Sweeney, J.A., Li, T., Gong, Q., 2009. Association of cerebral deficits with clinical symptoms in antipsychotic-naive first-episode schizophrenia: an optimized voxel-based morphometry and resting state functional connectivity study. Am J Psychiatry 166, 196-205.

McIntosh, A.R., 1999. Mapping cognition to the brain through neural interactions. Memory 7, 523-548.

McKeown, M.J., Makeig, S., Brown, G.G., Jung, T.P., Kindermann, S.S., Bell, A.J., Sejnowski, T.J., 1998. Analysis of fMRI Data by Blind Separation Into Independent Spatial Components. Hum.Brain Map. 6, 160-188.

McKeown, M.J., Sejnowski, T.J., 1998. Independent component analysis of fMRI data: examining the assumptions. Hum.Brain Map. 6, 368-372.

McKeown, M.J., Varadarajan, V., Huettel, S., McCarthy, G., 2002. Deterministic and stochastic features of fMRI data: implications for analysis of event-related experiments. J.Neurosci.Methods 118, 103-113.

Muller, J.L., Roder, C., Schuierer, G., Klein, H.E., 2002a. Subcortical overactivation in untreated schizophrenic patients: a functional magnetic resonance image finger-tapping study. Psychiatry Clin Neurosci 56, 77-84.

Muller, J.L., Roder, C.H., Schuierer, G., Klein, H., 2002b. Motor-induced brain activation in cortical, subcortical and cerebellar regions in schizophrenic inpatients. A whole brain fMRI fingertapping study. Prog Neuropsychopharmacol Biol Psychiatry 26, 421-426.

Nuechterlein, K.H., Dawson, M.E., Green, M.F., 1994. Information-processing abnormalities as neuropsychological vulnerability indicators for schizophrenia. Acta Psychiatr Scand Suppl 384, 71-79.

Raichle, M.E., MacLeod, A.M., Snyder, A.Z., Powers, W.J., Gusnard, D.A., Shulman, G.L., 2001. A default mode of brain function. Proc.Natl.Acad.Sci.U.S.A 98, 676-682.

Rissanen, J., 1983. A universal prior for integers and estimation by minimum description length. Ann.of Statistics 11, 416-431.

Saccuzzo, D.P., Braff, D.L., 1981. Early information processing deficit in schizophrenia. New findings using schizophrenic subgroups and manic control subjects. Arch Gen Psychiatry 38, 175-179.

Schmithorst, V.J., Holland, S.K., 2004. Comparison of three methods for generating group statistical inferences from independent component analysis of functional magnetic resonance imaging data. J.Magn Reson.Imaging 19, 365-368.

Smith, S.M., Fox, P.T., Miller, K.L., Glahn, D.C., Fox, P.M., Mackay, C.E., Filippini, N., Watkins, K.E., Toro, R., Laird, A.R., Beckmann, C.F., 2009. Correspondence of the brain's functional architecture during activation and rest. Proc Natl Acad Sci U S A 106, 13040-13045.

Talairach, J., Tournoux, P., 1988. A co-planar sterotaxic atlas of a human brain. Georg Thieme Verlag, Thieme, Stuttgart.

Vercammen, A., Knegtering, H., den Boer, J.A., Liemburg, E.J., Aleman, A., Auditory Hallucinations in Schizophrenia Are Associated with Reduced Functional Connectivity of the Temporo-Parietal Area. Biol Psychiatry.

Whitfield-Gabrieli, S., Thermenos, H.W., Milanovic, S., Tsuang, M.T., Faraone, S.V., McCarley, R.W., Shenton, M.E., Green, A.I., Nieto-Castanon, A., LaViolette, P., Wojcik, J., Gabrieli, J.D., Seidman, L.J., 2009. Hyperactivity and hyperconnectivity of the default network in schizophrenia and in first-degree relatives of persons with schizophrenia. Proc Natl Acad Sci U S A 106, 1279-1284.

Williamson, P., 2007. Are anticorrelated networks in the brain relevant to schizophrenia? Schizophr Bull 33, 994-1003.